Front. Chem. Sci. Eng. 2025, 19(5): 40
https://doi.org/10.1007/s11705-025-2541-6

REVIEW ARTICLE

State-of-the-art polymeric membranes and polymer derived membranes for simultaneous CO_2 and H_2S removal from sour natural gas

Luxin Sun[1,2], Qixuan Li[1,2], Kunying Li[1,2], Jiachen Chu[1,2], Yongsheng Li[1,2], Mengtao Wang[1,2], Zan Chen (✉)[3], Xiaohua Ma (✉)[1,2], Shouliang Yi (✉)[4,5]

1 State Key Laboratory of Separation Membranes and Membrane Processes, Tianjin 300387, China
2 School of Materials Science and Engineering, Tiangong University, Tianjin 300387, China
3 Key Laboratory of Membrane and Membrane Process, China National Offshore Oil Corporation Tianjin Chemical Research & Design Institute, Tianjin 300131, China
4 U.S. Department of Energy, National Energy Technology Laboratory, Pittsburgh, PA 15236, USA
5 Department of Civil and Environmental Engineering, University of Pittsburgh, Pittsburgh, PA 15261, USA

Abstract Natural gas is an important resource that ensures the energy supply and reduces CO_2 emissions simultaneously. However, many natural gases from well head contain a certain amount of acid gas, which must be removed to meet the pipeline requirement. Among the existing natural gas sweetening process, membrane technology is considered as a cost-effective, less energy intensive method that can remove both CO_2 and H_2S simultaneously. The membranes with high permeability, high selectivity, and good durability are developing very fast. In this review, we summarized the latest state-of-the-art membranes investigated for H_2S/CH_4 and CO_2/CH_4 separation applications, including conventional polymer membranes, polyimides, polymer of intrinsic microporosity, rubber polymers, carbon molecular sieve membranes, hollow fiber membranes, and membrane processes for H_2S and CO_2 removal from natural gas.

Keywords natural gas purification, H_2S removal, CO_2 capture, membranes, hollow fiber

1 Introduction

The excessive greenhouse gas emissions by human activities have resulted in a rapid increase in CO_2 content in the atmosphere, thus, causing serious environmental and ecological problems that have attracted global concern. Green, renewable energy is in high demand to meet the carbon capture and storage target for different countries [1,2]. Natural gas (NG) is considered the most feasible choice to fulfill the energy consumption increment and CO_2 emission reduction simultaneously, because the CO_2 generated by NG is about of coal burning based on the same calorific value [3]. Recently, there has been a rapid growth in NG consumption (Fig. 1) and the total amount reached 595 billion cubic meters in 2021 [4]. Meanwhile, over the past 10 years, the primary energy consumption ratio among coal, NG, oil, hydroelectricity, nuclear power, and renewable energies has changed, contrary to the intensive CO_2 emissions from coal and oil, the NG is the only primary energy source that are continuously increasing (Figs. 1(a) and 1(b)) from 22.4% to 24.4%.

At present, there is an urgent need to develop new technologies to improve NG production efficiently [5]. Generally, raw NG from well head contains CH_4 (70%–90%) and various associate components, including acid gases (major CO_2 and H_2S), water, and a certain amount of highly condensable hydrocarbons [6]. About 40% of the global NG contains a certain amount of H_2S and CO_2, and in some cases, the H_2S percentage can reach up to 23 mol % [7]. The acid gases should be removed to increase the calorific value of NG and reduce the pipeline corrosion, e.g., the pure CH_4 has a calorific value of 9100 kcal·m^{-3}, and the biogas, which contains 35%–40% of CO_2, only has the calorific value of 4800–6900 kcal·m^{-3} [8]. Furthermore, CO_2 needs to be

Received December 2, 2024; accepted February 9, 2025;
online March 25, 2025

E-mails: chenzan1018@163.com (Chen Z.),
xhuama@tiangong.edu.cn (Ma X.),
Shouliang.Yi@hotmail.com, Shouliang.Yi@pitt.edu (Yi S.)

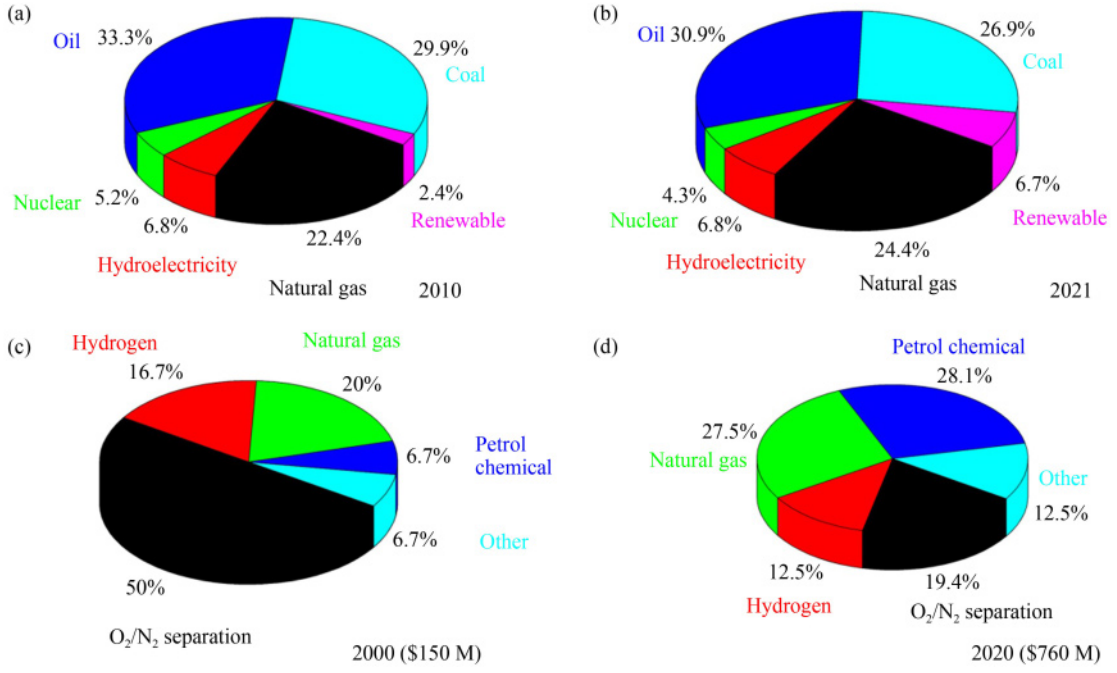

Fig. 1 (a) The ratio of different primary energies consumed in 2010. (b) The ratio of different primary energies used in 2021. The market value of membranes for different separation applications in (c) 2000 and (d) 2020. Reprinted with permission from Ref. [5], copyright 2008, American Chemical Society.

separated to less than 2% to reduce the corrosion of the pipeline [9]. On the other hand, H_2S has a foul oder of rotten eggs, and the removal of sulfur impurities from NG is also called "sweetening". H_2S removal is widely present in NG processing, petroleum refineries and geothermal energy production, posing significant public health concerns when released into the atmosphere. Apart from the unpleasant smell, H_2S is highly toxic as a gas by itself [10]. Very low concentrations of H_2S can be harmful or fatal to human beings. The LC50 is 800 ppm per 5 min [11], which must be decreased down to 4 ppm in NG to meet the pipeline requirement for safety transportation [5], whereas fuel cell applications typically need even lower H_2S content to less than 1 ppm [12].

One technique widely used in industrial for NG sweetening is scrubbing with diethanolamine (amines), sulfinol® (amines), rectisol® (methanol) or selexol™ (polyethylene glycol, PEG) that can combine/dissociate with CO_2 and H_2S by physical interactions [13,14]. This is plausible the most stable way to decrease the H_2S concentration below 4 ppm. However, the regeneration of these amines or alcohols is very energy intensive, meanwhile, the corrosion of the amine on the apparatus also makes other alternative methods very attractive. Membrane technology, a method without phase-change, offers several advantages such as a small footprint, cost-effectiveness, easy scalability, and continuous processing during separation, is developing rapidly in the industrial removal of acid gases [15]. Rezakazemi et al. [16] compared with the economics of CO_2 and H_2S removal from NG by absorption, membrane, and hybrid process, which is shown in Fig. 2. The results indicated that if the flow rate is less than 100 million standard cubic feet per day (MMSCFD), and the acid gas concentration is above 5%, membrane-based acid gas removal is considered as the most economical method. He also pointed out that for H_2S separation, the rubber polymers showed more competition for highly concentrated H_2S containing NG than glassy polymers. For CO_2 removal, glassy polymers are much better than the rubber polymers.

Here is the roadmap of membranes used for NG and biogas upgrading (Fig. 2(c)). In 1982, UOP pioneered in application of cellulose triacetate (CTA) membrane for CO_2/CH_4 gas pair separation [17]. Almost at the same time, Cynara tried to use CTA hollow fiber membranes for CO_2 removal in NG, and consequently, used for enhanced oil recovery [18]. Medel (now part of air liquide) and UBE also pioneered in PI membranes for CO_2 removal from NG or biogas [19]. In the 1990s, a large number of pilot scale offshore NG sweetening plants were established and the largest capacity can reach as much as 1280 MMSCFD, which was operated by Cynara in the Gulf of Thailand [20]. Recently, more than 130 biogas upgrading stations were built by Evonik, using PI membrane to upgrade NG and capture CO_2 at the same time [21].

The scope of this review is focused on the recent advances in polymers and their modified membranes for CO_2 and H_2S separation applications. Because there are plenty of reviews already for CO_2 removal from NG recently [15,22–29]. Herein, this review focuses more on the H_2S and CO_2 removal using membranes

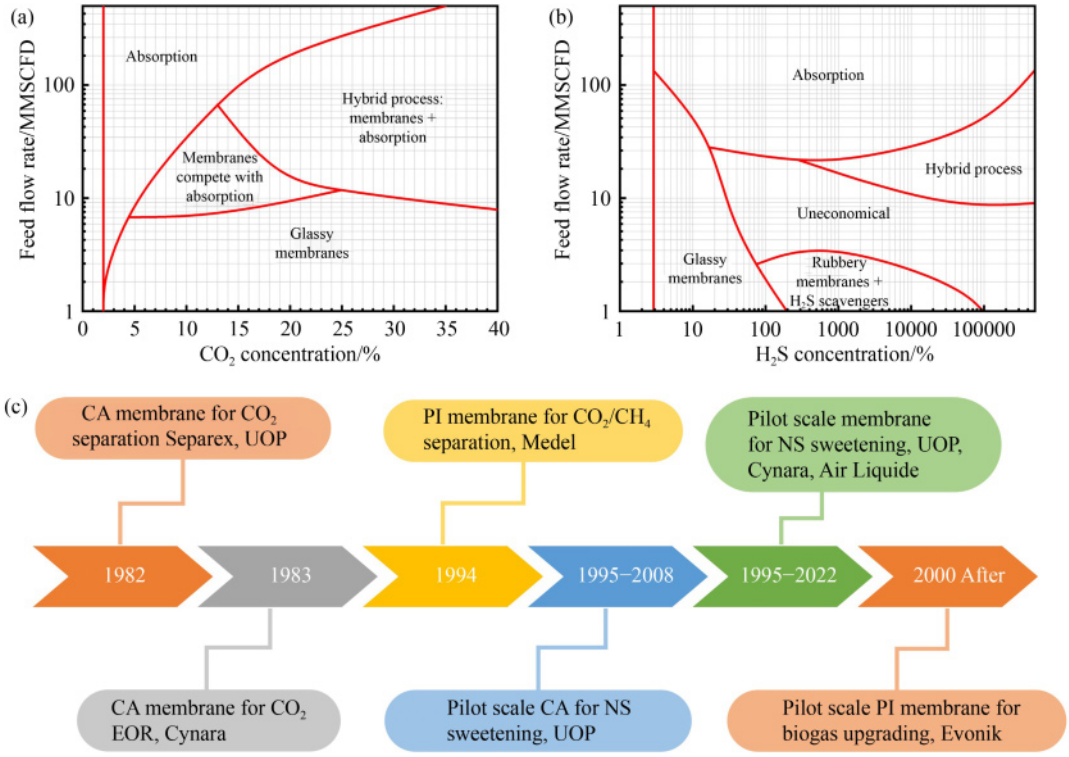

Fig. 2 The economic analysis of membrane, adsorption and combined methods for (a) CO_2 and (b) H_2S removal from NG; (c) road map of membrane based NG sweetening (CA: cellulose acetate; PI: polyimide; UOP: Universal Oil Products Company; EOR: enrichment of oil recovery).

simultaneously. The membranes ranging from conventional polymers, PIs, some specially designed polymers, carbon molecular sieve membranes (CMSMs), and the hollow fiber membranes as well as membrane processes are also summarized.

2 Background

2.1 Theory and gas transport mechanism

Gas separation membranes selectively transport gas molecules based on their different speeds, which is closely related to the properties of the polymer and the gas molecules. Typically, the dynamic diameter sequence of commonly used gas molecules is CH_4 (3.8 Å) > N_2 (3.64 Å) > O_2 (3.46 Å) > CO_2 (3.3 Å) > H_2 (2.89 Å) > He (2.6 Å) [30]. In general, the mechanisms of gas transport across the membrane can be categorized into Knudsen diffusion, molecular sieving and solution diffusion [31]. In polymer membranes, the gases permeate through the dense polymer membranes following the solution-diffusion model (Fig. 3(a)), in which, the gas first dissolves upstream of the membrane, and then, diffuses through the membrane toward downstream under pressure, and finally, desorption at the downstream surface of the membrane [32]. Separation of gases is achieved due to their differences in their rates of crossing the membrane.

According to Fick's law, the amount of gas movement is proportional to the concentration gradient. The diffusion flux of gas in the membrane can be expressed by q:

$$q = -D\frac{\mathrm{d}c}{\mathrm{d}x} = -D\frac{\Delta c}{\Delta x}, \tag{1}$$

where q is the flux of gas through the membrane, D is the diffusion coefficient ($cm^2 \cdot s^{-1}$), dc/dx is the concentration gradient, and the negative means the concentration gradient are opposite to the mass transfer. When the steady-state is reached, the gas concentration in the film becomes consistent. After integration of Eq. (1), the Eq. (2) can be obtained:

$$q = -\frac{D(c_1 - c_2)}{l}, \tag{2}$$

where l is the thickness of the membrane, c_1 and c_2 are the gas concentrations upstream and downstream of the membrane, respectively.

The solubility of gas in the membrane follows Henry's law, there is a proportional relationship between concentration c and gas partial pressure P, and the proportional constant is called the dissolution coefficient [33,34], denoted by S:

$$c = S \times p. \tag{3}$$

When put Eq. (3) into (2), we can get:

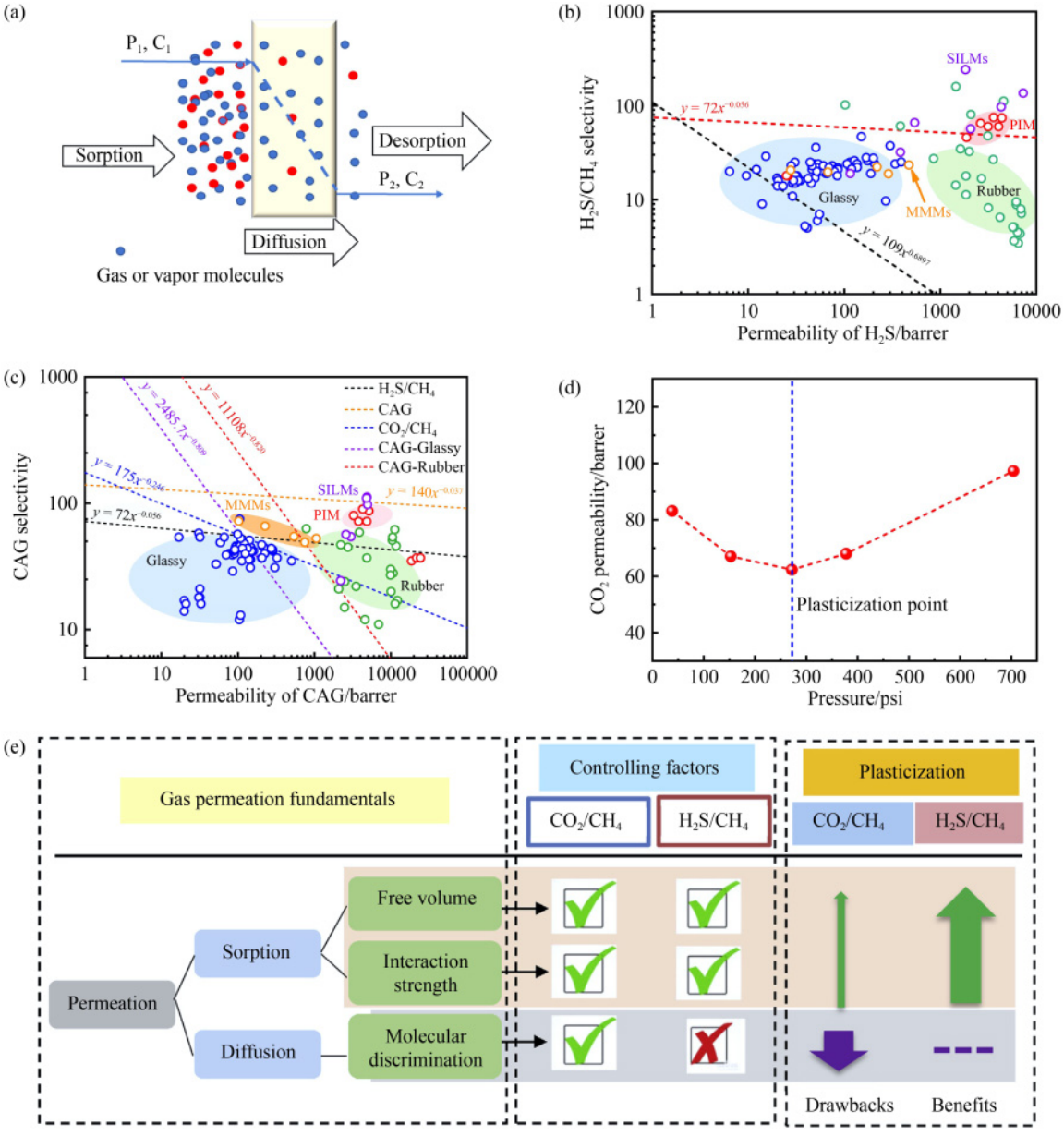

Fig. 3 (a) Proposed solution-diffusion mechanism of the gas transport through polymer membranes. (b) H_2S/CH_4 pure-gas trade-off curves for different types of polymers. (c) CAG (CO_2 + H_2S)/CH_4 and binary gas trade-off curves for different types of polymers. Reprinted with permission from Ref. [40], copyright 2019, American Association for the Advancement of Science, and Ref. [41], copyright 2021, Elsevier. (d) Plasticization effect and plasticization pressure of the polymer membranes as the pressure of CO_2 increase. (e) Plasticization effect on H_2S/CH_4 and CO_2/CH_4 separation properties. Reprinted with permission from Ref. [43], copyright 2020, Elsevier.

$$q = -\frac{D \times S \times (p_1 - p_2)}{l}. \quad (4)$$

The permeability coefficient is the combination of diffusion coefficient and dissolution coefficient, which is expressed by P [32]:

$$P = D \times S, \quad (5)$$

$$q = -\frac{P \times (p_1 - p_2)}{l}. \quad (6)$$

The permeability P_i of gas i can be determined by flux of the gas, membrane thickness l and transmembrane partial pressure ΔP (Eq. (6)), in barrer:

$$1\ \text{barrer} = 10^{-10}\ \frac{\text{cc(STP)} \cdot \text{cm}}{\text{cm}^2 \cdot \text{s} \cdot \text{cmHg}}. \quad (7)$$

The factors affecting the gas diffusion coefficient are as follows: (1) size and shape of gas molecules. In general, the larger the dynamic diameter of the gas, the smaller D; (2) flexibility of the polymer chain, the more flexibility of the polymer chains, the easier to move [35]; (3) fractional free volume (FFV, V_f) of the polymer. The FFV can affect

its diffusion coefficient, which can be expressed by the following equation:

$$D = A_0 \times \exp\left(-\frac{\gamma \times V^*}{V_f}\right), \quad (8)$$

where A_0 is a pre-exponential constant, which is related to the kinetic rate and molecular size of the gas, V^* is the critical free volume of the gas molecule, γ is the correction factor, V_f is the FFV of the polymer membrane, and can be calculated using the following Eq. (9):

$$V_f = V - V_0 = V - 1.3V_w, \quad (9)$$

where V_w is the van der Waals volume of the polymer, which can be calculated by the Bondi's group contribution method [36], V is the specific volume of the polymer that can be obtained by measuring the density of polymer.

The selectivity (α) of membrane between two different gases can be expressed by their permeation difference, shown as follows:

$$\alpha = \frac{P_A}{P_B} = \frac{D_A}{D_B} \times \frac{S_A}{S_B}, \quad (10)$$

where α is equal to the ratio of the two gas permeability coefficients, D_A/D_B is the diffusion selectivity, and S_A/S_B is the solubility selectivity.

2.2 Trade-off lines for CO_2/CH_4 and H_2S/CH_4 separation

For a special gas pair, there is a trade-off curve between gas permeability and gas pair selectivity. The correlation between single gas permeability and idea selectivity is:

$$P = k \times \alpha^n. \quad (11)$$

Freeman et al. [37] theoretically analyzed this trade-off effect and pointed out the relationships between the pre-exponential parameter (k) and power parameter (n) can be expressed as the following Eqs:

$$-\frac{1}{n} = \left(\frac{d_j}{d_i}\right)^2 - 1, \quad (12)$$

$$k^{-\frac{1}{n}} = \left(\frac{S_i}{S_j}\right) \times S_i^{-\frac{1}{n}} \times \exp\left\{\frac{1}{n}\left[b - f \times \left(\frac{1-a}{R \times T}\right)\right]\right\}, \quad (13)$$

where n is related to the kinetic diameters of gas molecules, the k is related to the rigidity of the polymer chain.

To better evaluate the gas separation performance of membranes, researchers constantly generate a variety of trade-off lines. However, the H_2S/CH_4 separation trade off curves is a special case, because the H_2S/CH_4 separation results reported in literatures largely depend on testing conditions such as pressure and component ratios. The trade-off curves for CO_2/CH_4 separation were proposed by Robeson based on conventional polymers and then updated by the appearance of PIM-1 (polymer of intrinsic microporosity) in 2008 [30,38]. However, it was re-defined in 2019 by Mckeown's group by the invention of a series of novel advanced PIMs [39]. As for the H_2S/CH_4 gas pair, George et al. [25] analyzed different membranes for acid gas removal from NG, and found that there are some trade-off effects between the H_2S permeability and H_2S/CH_4 selectivity but not specified. Later, the trade-off curve was proposed by Yi et al. [40] and Hayek et al. [41] separately from some state-of-the art polymer membranes at tri-component acid gas conditions and different pressures. Their trade-off lines and the fitted n and k parameters are shown in the following Figs. 3(b) and 3(c) and Table 1. The result indicated that they are different to a large extent based on different polymers as standard.

Kraftschik et al. [42] introduced a new criterion to assess the overall acid gas sweetening performance of polymeric membranes in sour mixed-gas separation conditions for both H_2S and CO_2. The overall acid gas removal properties of membranes are the combined permeability of H_2S and CO_2, and the approximate selectivity coefficients are the sum of H_2S/CH_4 and CO_2/CH_4 selectivity. As shown in the following equations.

$$P_{CAG} = P_{H_2S} + P_{CO_2}, \quad (14)$$

$$\alpha_{CAG} = \frac{P_{H_2S} + P_{CO_2}}{P_{CH_4}}. \quad (15)$$

2.3 Plasticization effect of CO_2 and H_2S in membrane-based NG sweetening

The gas separation properties of polymer membranes suffer from the plasticization effect, which originated from the average chain distance of the polymer chains become larger than its prototype under high pressure of condensable gases or vapors, and thereafter, enhances its permeability whereas decreases their gas pair selectivity [44–46]. In real NG separation conditions, the upstream pressure of the mixture can be as much as 800–1000 psi, and the partial pressure for both CO_2 and H_2S can be over 10 atmosphere pressure. The plasticization is a very common phenomenon in NG sweetening, especially for CO_2/CH_4 and H_2S/CH_4 separations. The point at which

Table 1 The fitted n and k parameters of the trade-off curves for CO_2/CH_4, H_2S/CH_4 and combined acid gas (CAG) removal

Proposed upper bond	Ref.	k	n
CO_2/CH_4	[39]	1.31×10^9	–4.065
H_2S/CH_4	[41]	2.391×10^{35}	–18.868
	[40]	898	–1.45
CAG	[41]	1.95×10^9	–4.13
	[40]	1.57×10^4	–1.23
	[40]	8.58×10^4	–1.22

this happens is called the "plasticizing pressure", as illustrated in Fig. 3(d). Numerous investigations have explored how to alleviate the plasticization effect, such as thermal annealing, physical and chemical crosslinking [47−49]. All these approaches can significantly reduce the plasticization effect of CO_2 to some extent. However, the H_2S has a higher critical temperature (373.5 K) than CO_2 (304.2 K), which has a higher solubility coefficient than CO_2, under the same pressure, the H_2S will induce a more serious plasticization effect. Meanwhile, the kinetic diameter of H_2S (3.62 Å) is closer to CH_4 (3.84 Å) than that of CO_2 (3.3 Å, Table 2), this will lead to a much smaller diffusion selectivity of H_2S/CH_4 than that of CO_2/CH_4, as a result, the H_2S/CH_4 separation is more dependent on solubility selectivity whereas the CO_2/CH_4 separation relay on both solubility and diffusion selectivity. The plasticization for CO_2/CH_4 resulted in a huge decreased selectivity, however, the plasticization can improve both the H_2S permeability but also H_2S/CH_4 selectivity due to the sorption effect (Fig. 3(e)) [43].

3 Dense membrane for H_2S removal from NG

Polymeric membranes are the most successful membranes in industrial applications for H_2S separation due to their high chemical stability, robustness, and flexibility in bulk separation, applicable to both high and low levels of H_2S. The effectiveness of H_2S removal by these membranes depends on their chemical and physical structures, and thus, a large number of polymers have been reported for H_2S and CO_2 removal. Here, membranes such as glassy polymer membranes, rubber polymer membranes, and carbon molecular sieving membranes are summarized.

3.1 Glassy polymers for H_2S removal from NG

Glassy polymers are a kind of polymers that have their glass transition temperatures (T_g) above room temperature [51]. Due to the rigidity, good film formability, modest permeability, high selectivity for CO_2/CH_4 and can simultaneously remove H_2S, which is widely investigated as membranes for separation applications. Thousands of glassy polymers are synthesized for sweetening of NG, and these polymers can be classified into polysulfone (PSF), CA, polycarbonate, polyphenylene oxide (PPO), PI, PIMs, and their modified polymer membranes.

Table 2 Relevant physical properties of H_2S, CO_2, and CH_4

Gas	Kinetic diameter/Å [50]	Lennard-Jones temperature/K [50]	Critical temperature (T_c)/K [31]
H_2S	3.62	301	373.5
CO_2	3.32	195	304.2
CH_4	3.82	149	190.5

3.1.1 CA for H_2S and CO_2 separation

Cellulose is a polysaccharide consisting of a linear chain with hundreds to thousands of β-(1,4)-linked D-glucose units, which is the most abundant organic material in nature. Cellulose can be made into celluloid, paper, cloth, and consumables, pharmaceuticals, and so on [52]. CA membranes have been extensively used for acid gas removal from natural or biogas since the mid-1980s, representing ~80% share in the NG processing membrane market [53]. There are different types of CA membranes, depending on the acetyl group substitution content (Fig. 4(a)). The prototype is CA. The strong hydrogen bonding and high crystallinity prevent gas molecules from permeating. The commonly used one is CTA with acetyl groups concentration of ~2.84 [54]. Considering its low cost, high stability and good vapor resistance, CTA membrane was chosen for NG sweetening for a long period. In 1989, Schell et al. [55] reported the CO_2 and H_2S separation performance of CTA in the presence of concentrated CO_2 and H_2S with the component ratio of $CH_4/CO_2/H_2S$ (38/45/17) at 200 psi, a modest selectivity of 10–14 for CO_2/CH_4 and 15–20 for H_2S/CH_4 were obtained during 1500 h of testing (Table 3). Chatterjee et al. [56] reported the selectivity and permeability of CTA for CO_2/CH_4 and H_2S/CH_4 under a mixed-gas ($CH_4/CO_2/H_2S$ = 65/29/6) feed pressure of 10 bar. The dense CTA membrane has a pretty low CO_2 and H_2S permeability of ~2.4 barrer of each, combined with very close CO_2/CH_4 and H_2S/CH_4 selectivity of 22.1 and 19.4, respectively. Crosslinking of the CTA is a good method to improve its CO_2 and H_2S separation properties, because crosslinking can disrupt its crystallinity, enhance permeability, and improve resistance to plasticization simultaneously. Achoundong et al. [57] reported a series of vinyltrimethoxysilane (VTMS) modified CTA to adjust its H_2S and CO_2 separation performances as well as the membrane plasticization resistance (Fig. 4(a)). The resulting crosslinked CTA membranes showed a slightly higher H_2S/CH_4 (34.3 *vs.* 29.7) and similar CO_2/CH_4 selectivity of 21 than the pristine CTA membrane under high gas feed pressure of 500 psi with $CH_4/CO_2/H_2S$ component ratio of 60/20/20, however, the CO_2 and H_2S permeabilities are more than 10 times higher than the neat CTA membrane, that is, 204 *vs.* 8.71 barrer for H_2S and 129 *vs.* 8.66 barrer for CO_2 (Table 3). Meanwhile, under the upstream pressure of 700 psi in a ternary $CH_4/CO_2/H_2S$ (60/20/20) mixture, the VTMS-modified CA membranes showed a high H_2S/CH_4 (~28) and CO_2/CH_4 (~20) selectivity, and pretty high H_2S and CO_2 permeability of above 190 and 136 barrer, respectively. The VTMS-modified CTA demonstrated a very

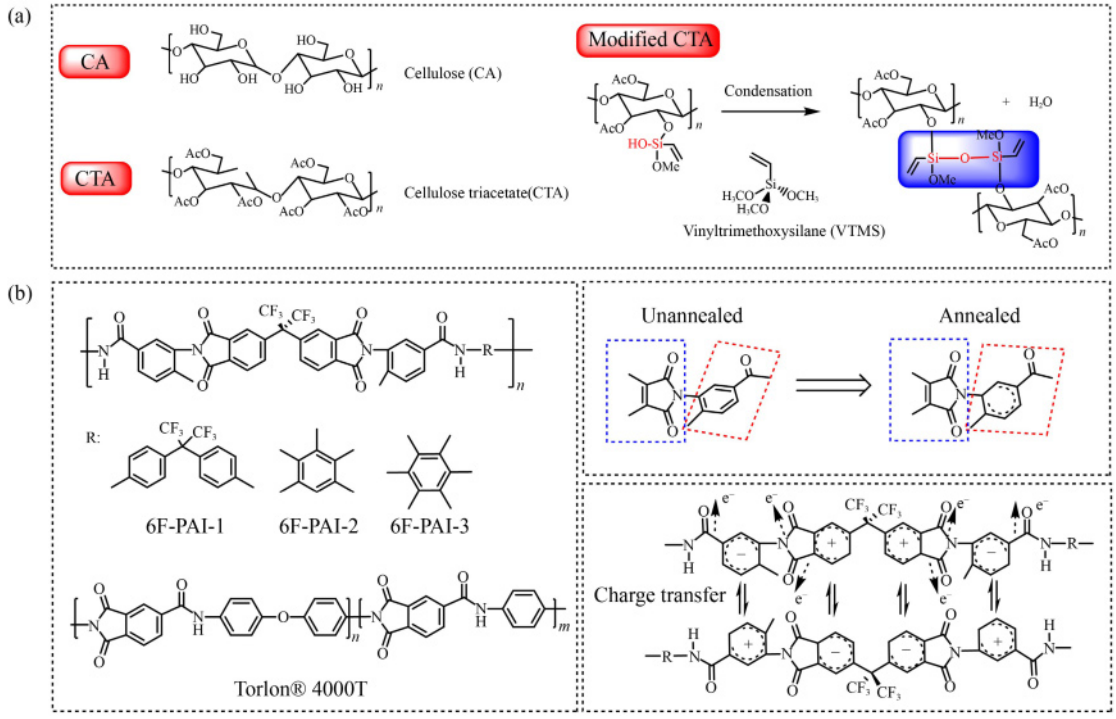

Fig. 4 (a) Structures of CA, CTA and modified CTA. (b) Chemical structures of the polyamide-imide (PAI) for H_2S and CO_2 removal from NG. The effect of annealing on the imide bond and charge transfer of the PAI main chain are also illustrated.

Table 3 Gas permeation properties of CTA at 35 °C

Condition	Feed gas conditions M ($CH_4/CO_2/H_2S$)[a)]	P_{CO_2} [b)]	P_{H_2S} [b)]	P_{CO_2}/P_{CH_4}	P_{H_2S}/P_{CH_4}	Ref.
CTA	M (38/45/17), 200 psi			10–14	15–20	[55]
CA	M (65/29/6), 145 psi	2.43	2.13	22.1	19.4	[56]
CA	M (60/20/20), 500 psi	8.66	8.71	29.5	29.7	[57]
	M (60/20/20), 700 psi	27.5	37.9	19.1	27.4	
VTMS-modified CTA	M (60/20/20), 500 psi	129.4	204	21.8	34.3	[57]
	M (60/20/20), 700 psi	136	190	20	27.5	
CA	Humid CO_2/H_2S (5/15)	51.4	65.2	14.7	18.7	[58]
CA	CO_2/H_2S (5/15), stage cut 1.5% (humid gas)	58.2	79.8	17.0	23.4	
	CO_2/H_2S (5/15), stage cut 10% (dry gas)	54.2	68.2	14.5	18.2	
	CO_2/H_2S (5/15), stage cut 1.5% (dry gas)	61.6	80.7	17.0	22.3	

a) Feed conditions; b) permeability of the membranes, unit, barrer, 1 barrer = 10^{-10} $cm^3 \cdot cm \cdot cm^{-2} \cdot s^{-1} \cdot cmHg^{-1}$.

promising NG sweetening potential for removing CO_2 and H_2S at the same time.

Recently, removing H_2S and CO_2 from humidified and hydrocarbon contained NG was reported by Peters et al. [58], who studied the stability of CTA dense membranes in humid NG feed streams with a ternary $CH_4/CO_2/H_2S$ feed component ratio of (80/5/15). Meanwhile, there are trace amounts of butane and toluene up to 4500 ppm. The CTA membranes were evaluated at 30 and 50 °C in the pressures of 20, 35, and 50 bar. The results showed that the introduction of butane and toluene in the high H_2S feed mixture resulted in an inhibition of both the CO_2 and H_2S permeability, which is ascribed to the highly condensable gases not only competing with H_2S and CO_2 by sorption but also hinder their diffusion. However, after a period of equilibrium region, the CTA membranes demonstrated excellent stability even when the testing time was extended to 800 h.

3.1.2 PAI for H_2S and CO_2 separation

PI is a kind of aromatic heterocyclic polymer containing an imide group in the main chain, known for its excellent heat resistance, electrical insulation properties, chemical resistance and mechanical strength. So, they are widely used in gas separation fields [59−66]. PI is synthesized by the polycondensation of diamine and dianhydride, their properties can be fine-tuned by changing the structure and component ratios of the monomers. By sophisticated design, PIs are often used in NG sweetening both in academic and real industrial [67−72]. Among them, PIs based on 4,4'-(hexafluoroisopropylidene) diphthalic

anhydride (6FDA) have received widespread attention due to their ease of solution processing, relatively good thermal and chemical stability, and excellent mechanical properties. In addition, the presence of a bulky CF_3 group in the PI main chain also results in high free volume and enhances chain stiffness, as a result, 6FDA derived PIs exhibit high selectivity and permeability as compared to conventional PIs. However, 6FDA-based PIs are susceptible to plasticization, especially in the presence of H_2S. To mitigate the H_2S and CO_2 plasticization behavior of 6FDA-based PIs, an amide bond (–CO–NH–) with strong hydrogen bonding was introduced to form PAI to enhance the inter- and intra-molecular interaction. For example, Vaughn et al. synthesized a series of 6FDA-based PAI membranes (6F-PAI-1, 6F-PAI-2, 6F-PAI-3) by reacting 6FDA with three diamines, and their structures are shown in Fig. 4(b) [73]. All membranes demonstrated much higher H_2S and CO_2 permeability than Torlon (Fig. 4(b)). For example, the 6F-PAI-1 showed an H_2S permeability of 6.2 barrer, which is 31 times higher than Torlon. After annealing at 200 °C for 24 h, although there was a slight decrease in CO_2 permeability, there is almost no plasticization till CO_2 pressure up to ~1000 psi. This is attributed to the annealing treatment promoting the intra- and intermolecular charge transfer (Fig. 4(b)) of the polymer main chain, and improved the plasticization resistance of the material to CO_2 and H_2S.

The 6F-PAI-1 showed higher stability in swelling than 6F-PAI-2 and 6F-PAI-3 when using pure H_2S gas as feed (5.5 *vs.* 7 bar). This is due to the reduced solubility of H_2S in a highly fluorinated polymer matrix. The concentration of H_2S in the feed gas also has a huge influence on the acid gas removal performances.

3.1.3 PI for H_2S and CO_2 separation

Vaughn and Koros [74] analyzed the H_2S, CH_4, and CO_2 transport properties of 6F-PI-1 membrane under two acid gas concentrations with H_2S rich $CH_4/CO_2/H_2S$ (60/20/20) and H_2S lean $CH_4/CO_2/H_2S$ (50/45/5) mixtures. The CO_2 permeability continuously decreased as the H_2S concentration increased but their CH_4 permeability changed very slightly as the H_2S concentration changed. At the same time, although the permeability of H_2S in the mixed-gas is lower than the pure-gas, the H_2S permeability in the H_2S rich mixed-gas is much higher than the H_2S lean condition and continuously increases as the partial pressure of H_2S increases (Figs. 5(a) and 5(b)). Surprisingly, the selectivity of H_2S/CH_4 gradually increased as the feed pressure increased in the H_2S rich feed gas whereas the H_2S/CH_4 continuously decreased in the H_2S lean mixed-gas till the feed pressure up to 800 psi (Fig. 5(c)). This is due to the competitive sorption that restricted the H_2S Langmuir sorption capacity in the large amount of CO_2 in the H_2S lean component, and thus, gives lower solubility selectivity of H_2S/CH_4.

Another way to improve the H_2S and CO_2 separation performance of PI is copolymerization. Copolyimides exhibit the advantages of different monomers, which can fine tune the H_2S and CO_2 removal performances from NG at the molecular level. For random copolymers, the properties can be adjusted by changing the proportion of different monomers. For block copolymers, their properties can be adjusted by varying the lengths and proportions of different blocks. Yahaya et al. [75] conducted an in-depth study on block copolyimide membranes based on (6FDA-mPDA (4,4'-m-phenylenediamine))-(6FDA-durene) for sour gas separation, which showed H_2S/CH_4 and CO_2/CH_4 selectivity of 23 and 27, respectively. The membranes demonstrate excellent stability and separation performance over a wide range of temperatures and pressures, maintaining high H_2S/CH_4 and CO_2/CH_4 separation factors even at H_2S concentrations up to 20 wt %. Notably, as the feed H_2S concentration and partial pressure increase, there is a reciprocal selectivity trend for CO_2/CH_4 and H_2S/CH_4, in which, the CO_2/CH_4 gradually decreases whereas the H_2S/CH_4 continuously increase in the opposite way. This is due to the highly condensable gases, such as CO_2 and H_2S, competing with each other for the sorption sites. Since H_2S has a higher affinity than CO_2 it greatly reduced the CO_2 solubility, leading to a lower CO_2 permeability. On the other hand, CH_4 is not greatly affected because of its much lower affinity for the sorption sites than both CO_2 and H_2S.

Later, Yahaya et al. [77] introduced the CARDO building block into random copolyimides to inhibit interchain stacking and intra-chain packing, the resulting membrane showed an increased permeability without reducing selectivity. In the multi-component feed gas mixtures with H_2S concentration up to 20 vol %, The 6FDA-durene/CARDO (1:3) ideal selectivity of CO_2/CH_4 and H_2S/CH_4 are 19–24 and 21–24, and the permeability of CO_2 and H_2S are 32–55 barrer and 46–53 barrer (Table 4), respectively. Alghannam et al. [78] conducted an in-depth study on the gas separation performance of block copolyimides using CARDO as a building block, who found that the block copolyimide 6FDA-CARDO/6FDA-durene membrane was highly stable in aggressive environments. Among them, 6FDA-CARDO/6FDA-durene (2500/2500) membrane performs well in harsh acidic gases (mixtures of CO_2, CH_4, N_2, C_2H_6, and H_2S), with H_2S permeability of 275.8 barrer and H_2S/CH_4 selectivity of 20.1 at 36 vol % H_2S and feed pressure of 27.6 bar. Hayek et al. [79] studied the gas separation performance of random and block copolyimides of 6FDA-6FpDA-durene, the results showed that block copolyimides performed better than random copolyimides in gas separation. When the 6FpDA/durene molar ratio changed from 25% to 80%, the ideal selectivity coefficient of CO_2/CH_4 increased to approximately 47, while the CO_2 permeability coefficient

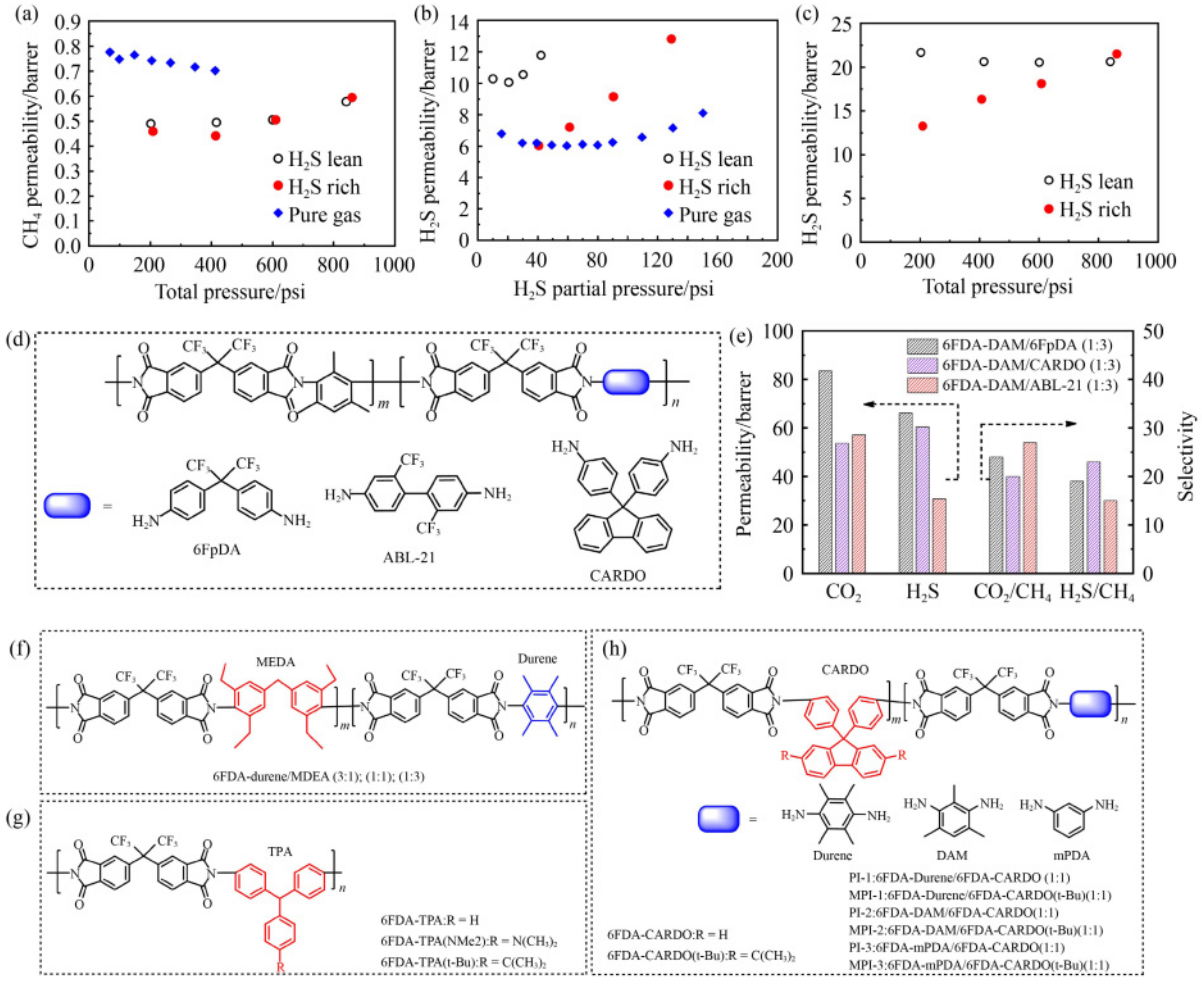

Fig. 5 Pressure-dependent permeability for (a) CH_4, and (b) H_2S under pure-gas, H_2S lean and H_2S rich mixed-gas conditions from low to high pressure. (c) Pressure-dependent H_2S permeability and H_2S/CH_4 selectivity under H_2S lean and H_2S rich conditions. Reprinted with permission from Ref. [74], copyright 2014, Elsevier. (d) The structure of PIs (6FpDA: 2,2-bis(4-aminophenyl) hexafluoropropane). (e) Sour mixed-gas CO_2 and H_2S permeability coefficients and CO_2/CH_4 and H_2S/CH_4 selectivity. Reprinted with permission from Ref. [76], copyright 2021, Elsevier. Chemical structure of PI for NG sweetening with bulky groups. (f) Substitution in the main chain using 4,4'-methylene benzene (2,6-diethylaniline) (MDEA) as a monomer. (g) Substitution in the side chain using 4,4'-diaminotriphenylamine as a building block. (h) Substitution using the CARDO and substituted CARDO as a building block.

gradually decreased to 65 barrer. Further increasing the content of 6FpDA to 80%, the mixed gas permeability of CO_2 decreased to 45 barrer coupled with CO_2/CH_4 selectivity of 39 for 6FDA-6FpDA/6FDA-durene (4:1) block copolyimide membrane. However, when the polymer was exposed to a gas mixture of $H_2S/CO_2/CH_4$ with 20 vol % H_2S content, the CO_2/CH_4 selectivity value dropped to approximately 20.8 and the H_2S/CH_4 selectivity coefficient was 13.1 at upstream pressures up to 500 psi. The permeability coefficients of CO_2 and H_2S were 41.7 and 26.4 barrer (Table 4), respectively.

Yahaya et al. [76] synthesized three random copolyimides using 6FDA with DAM (2,4,6-trimethyl-m-phylenediamine) and another three diamines of 6FpDA, CARDO, and ABL-21 at the ratio of 1:3 (Fig. 5(d)). Without H_2S in the feed gas, the 6FDA-DAM/6FpDA (1:3) random copolyimide membrane exhibited the highest CO_2 permeability of ~89 barrer and CO_2/CH_4 selectivity of ~35 at 55 bar. When the 20% H_2S was introduced, the CARDO-based diamine showed both higher H_2S permeability and H_2S/CH_4 selectivity than both the 6FpDA- and ABL-21-based diamines, however, the 6FpDA-based copolyimide showed the highest CO_2 permeability and also pretty high CO_2/CH_4 selectivity. As a result, the 6FDA-DAM/6FpDA (1:3) membrane showed the best CAG separation property, even at upstream pressures up to 34.5 bar at 25 °C (Fig. 5(e)). The block copolyimide of 6FDA-DAM/6FDA-CARDO (1:1) in sour mixed-gas condition showed much higher permeability than the random 6FDA-DAM/CARDO (1:3) copolyimide and also maintained high CO_2/CH_4 and H_2S/CH_4 selectivity. For example, the CO_2, and H_2S permeability coefficients increase about 57% and 93%, and the CO_2/CH_4 and H_2S/CH_4 selectivity only dropped

Table 4 CO_2/CH_4 and H_2S/CH_4 separation properties of PI membranes

Membrane	$P^{a)}$	$H_2S/CO_2/CH_4/N_2/C_2H_6$	$P_{H_2S}{}^{b)}$	$P_{CO_2}{}^{b)}$	P_{CO_2}/P_{CH_4}	P_{H_2S}/P_{CH_4}	Ref.
6F-PAI-1	900	10/20/70	4	8.1	32	17	[73]
	600	10/20/70	4	11.4	35	12	
6F-PAI-2	800	20/20/60	4	7.5	12	7	
	600	20/20/60	4	7.4	14	7	
(6FDA-mPDA)-(6FDA-durene) (5000/5000)	500	1/10/59/30	9.6	21.1	39	18	[75]
	500	10/10/60/20	6.4	10.9	34	20	
	500	20/10/60/10	15.3	15.6	29	29	
(6FDA-CARDO/durene) (1:3)	300	10/10/60/20	47.2	46.8	23	23	[77]
	450	10/10/60/20	48.9	43.3	21	24	
6FDA-CARDO/6FDA-durene (2500/2500)	200	36/10/48.6/4.4/1	162.5	100.2	15.2	24.7	[78]
	400	36/10/48.6/4.4/1	275.8	142.2	10.4	20.1	
6FDA-6FpDA/6FDA-durene (4:1)	350	20/10/59/10/1	24.4	42.0	23.6	13.7	[79]
	500	20/10/59/10/1	26.4	41.7	20.8	13.1	
6FDA-DAM/6FpDA (1:3)	349	20/10/57/10/3	52.7	69.6	28.0	21.2	[76]
6FDA-DAM/CARDO (1:3)	349	20/10/57/10/3	61.7	54.2	20.9	23.9	
6FDA-DAM/ABL-21 (1:3)	349	20/10/57/10/3	31.5	57.6	27.8	15.2	
6FDA-durene/MDEA (1:3)	400	20/10/59/10/1	135.6	87.7	16	24	[82]
6FDA-TPA	300	20/10/59/10/1	63.1	48.5	15	20	[83]
	500	20/10/59/10/1	85.6	60	15	21	
6FDA-TPA (t-Bu)	300	20/10/59/10/1	78.4	60.5	16	20	
	500	20/10/59/10/1	84.2	60.4	13	18	
6FDA-CARDO	300	22/10/55/10/3	26.5	26.0	22.3	22.7	[84]
6FDA-CARDO (t-Bu)	300	22/10/55/10/3	101	80.4	15.0	18.9	
6FDA-durene/6FDA-CARDO (t-Bu)	500	20/10/59/10/1	456	238	10.6	20.4	[85]
6FDA-DAM:DABA(3:2)_180C	900	5/0/95	32	–	–	18	[42]
6FDA-DAM:DABA(3:2)_230C	900	10/20/70	29.5	40	22	16	
	700	10/20/70	23	29	18	14	
6FDA-DAM:DABA (3:2)	700	25/5/70	106.7	97.73	22	24	[86]
6FDA-DAM:DABA (1:1)	700	25/5/70	27.87	37.99	31	23	
6FDA-DAM:DABA (1:2)	700	25/5/70	12.18	19.82	34	21	
6FDA-DAM	100	0.5/20/79.5	1076	737	26	39	[43]
	500	0.5/20/79.5	612	411	26	39	
DEGMC	900	20/20/60	43	55	22	18	[87]
TEGMC	900	20/20/60	43	50	29	25	
TetraMC	900	20/20/60	30	42	29	21	

a) Feeding pressure of the upstream gas; b) permeability of the membranes, unit, barrer.

23% and 6%, respectively. This performance exceeds that of glass polymers currently used in the industry, making this membrane a potential candidate for NG sweetening.

The bulky substitution of the diamine can also improve the H_2S/CH_4 separation performance of the PI membranes. MDEA has gained attention due to the steric hindrance provided by the tetraethyl-substituted benzene ring, which restricts the free rotation of the central methylene group [72,80,81]. Hayek et al. [82] reported the 6FDA-durene/MDEA random copolyimides with different molar ratios of durene and MDEA (3:1, 1:1, and 1:3), and studied their pure gas permeation properties. Compared to the pure PIs (6FDA-MDEA and 6FDA-durene, Fig. 5(f)), these copolyimides showed significant improvements in gas separation performance. For example, at a pure gas feed pressure of 100 psi, 6FDA-durene/MDEA (3:1) obtained the best CO_2 permeability of 234 barrer, and CO_2/CH_4 selectivity of 17.8. For a mixture consisting of 10% CO_2, 59% CH_4, 30% N_2, and 1% C_2H_6, 6FDA-durene/MDEA (1:3) showed a CO_2 permeability of 87.7 barrer and a CO_2/CH_4 selectivity of about 24 at elevated pressures of 400 psi (Table 4). On the other hand, the substitution at the pendent group also has a prominent effect on the CO_2 and H_2S separation properties of the resulting PI membrane, for example, Hayek et al. [83] introduced two large side groups, dimethylamino group and tert-butyl group, into 4,4'-diaminotriphenylamine-based PIs (Fig. 5(g)), and found that both side groups can increase the FFV in the polymer membrane matrix, thereby improving the gas diffusion, but the solubility coefficient is almost the same. Later, Hayek et al. [84] successfully introduced a tert-butyl group into the 6FDA-CARDO molecular structure through Friedel-Crafts alkylation reaction, which significantly increased the FFV of the resulting membrane material. The gas separation performance of 6FDA-CARDO (t-Bu) membrane was superior to that of 6FDA-CARDO. The 6FDA-CARDO (t-Bu) membrane showed an H_2S permeability of 148 barrer and an H_2S/CH_4 selectivity of 16.1 at 500 psi. Tert-butyl substituted CARDO-based copolyimides were also reported by using durene as the second diamine (Fig. 5(h)) [85]. The

resulting 6FDA-durene/6FDA-CARDO (t-Bu) demonstrates an H_2S and CO_2 permeability coefficients of 456 and 238 barrer, respectively, with selectivity of 20.4 for H_2S/CH_4 and 10.6 for CO_2/CH_4, which exceeds most glass PIs and has great hope in NG deacidification applications.

An industrial applicable membrane material must be highly efficient and stable in the desired separation. For high condensable gases such as CO_2 and H_2S, which often resulted in plasticization. In general, due to the higher condensability of H_2S over CO_2, it showed much lower plasticization pressure. However, the plasticization had a positive effect on both H_2S permeability and H_2S/CH_4 selectivity. For example, Kraftschik et al. [42] investigated the dense PI membranes by copolymerization of 6FDA-DAM/DABA (3,5-diaminobenzoic acid) with different ratios (3:2; 1:1; 1:2) for aggressive sour gas $H_2S/CO_2/CH_4$ (9.95/19.9/70.15) separations till high pressure. In which, the permeability of H_2S continuously increased as the pressure increased up to 300 psi (Fig. 6(a)), at the same time, the H_2S/CH_4 selectivity further enhanced from ~18 to 25 (Fig. 6(b)). On the other hand, the CO_2/CH_4 separation is totally different from H_2S separation, e.g., after plasticization, there is a huge improvement in CO_2 permeability (Fig. 6(c)), however, the CO_2/CH_4 selectivity gradually decreased to more than half till the upstream pressure of over 700 psi (Fig. 6(d)). Plasticization of PI is beneficial for H_2S/CH_4 separation by promoting sorption coefficient and selectivity. However, due to the loss of molecular sieve separation effect, it is not conducive to CO_2/CH_4 separation.

Crosslinking either physical or chemical is an efficient way to enhance the H_2S/CH_4 separation and anti-plasticization properties. The 6FDA-DAM/DABA (3/2) is a good candidate material due to its inherent chemical, mechanical, and thermal stability. In addition, the crosslinking capabilities of the COOH group in the PI provide a good way to improve resistance to plasticity and may even enhance the overall performance. Kraftschik et al. [42] introduced a COOH group in the PI backbone by reacting the DABA with 6FDA to form the 6FDA-DAM:DABA (3:2) membrane. The results show that the introduction of H_2S into the feed stream results in a significant difference in plasticization resistance. In pure H_2S, when the feed pressure is lower than 1 bar, the plasticizing effect occurs. Thermal annealing at sub T_g can effectively reduce the plasticizing effect. E.g., the ideal selectivity value for H_2S/CH_4 is 90% higher than that of binary and ternary gas penetration tests with H_2S partial pressure greater than 2 bar. Liu et al. [86] discovered that the increase in DAM ratio led to a higher plasticization tendency of 6FDA-DAM:DABA PI membrane. The increased DAM:DABA ratio can provide a higher H_2S permeability, while the H_2S/CH_4 selectivity

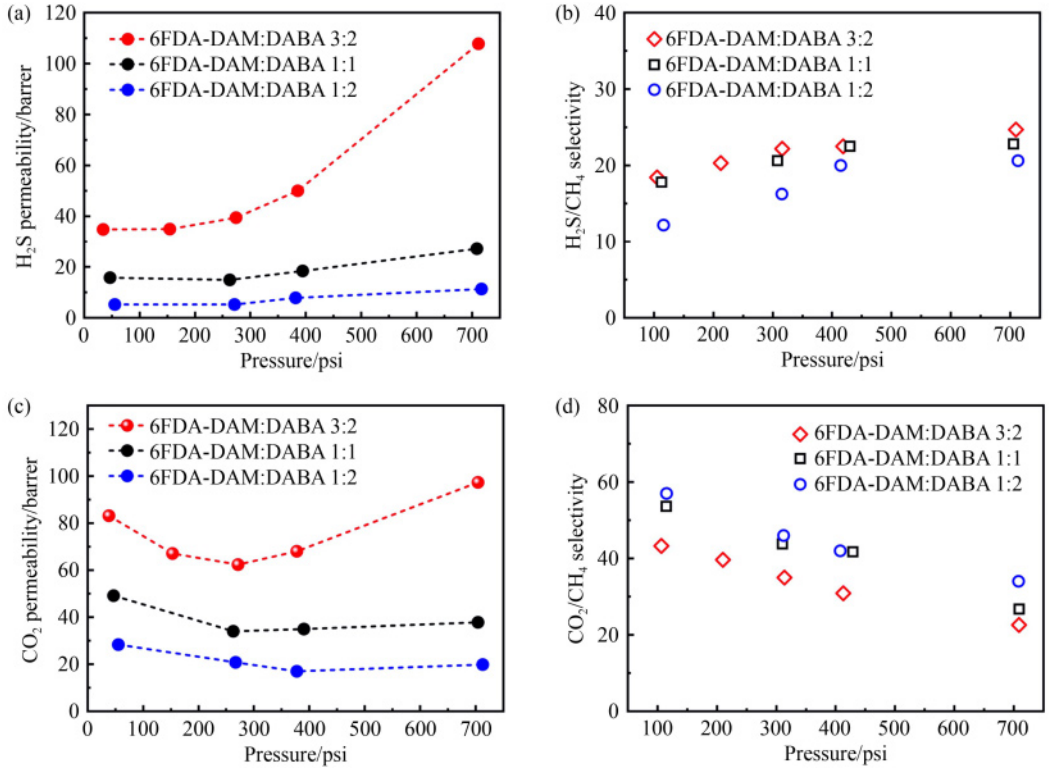

Fig. 6 H_2S and CO_2 separation performance of 6FDA-DAM/DABA membranes under ternary sour gas ($H_2S/CO_2/CH_4$ = 9.95/19.9/70.15) at 35 °C. (a, b) H_2S permeability and H_2S/CH_4 selectivity as a function of feed pressure. (c) CO_2 permeability and (d) CO_2/CH_4 selectivity as function of total pressure. Reprinted with permission from Ref. [86], copyright 2020, John Wiley & Sons, Inc.

is almost unchanged. They also reported the H_2S/CH_4 and CO_2/CH_4 separation performance of 6FDA-DAM and 6FDA-DAM/DABA (3:2) under various conditions [43], and found that when H_2S is present in the feed, PI membrane plasticization can actually provide a huge performance advantage for H_2S/CH_4 separation, while unfavorable to CO_2/CH_4 due to the loss of molecular sieve separation effect. For example, when a gas mixture ($H_2S/CO_2/CH_4$ = 20/20/60) was used as feed gas at 46 bar, the 6FDA-DAM shows an H_2S permeability of 495 barrer and H_2S/CH_4 selectivity of 31, and a CO_2 permeability of 301 barrer combined with CO_2/CH_4 selectivity ~19 (Table 4).

To improve the stability of the membrane, Kraftschik and Koros [87] prepared a series of crosslinked membrane materials based on the 6FDA-DAM:DABA (3:2) PI backbone. Short-chain PEG molecules are used as crosslinkers in esterification reactions from ~230 to 280 °C such as diethylene glycol (DEG), triethylene glycol (TEG) and tetraethylene glycol (TetraEG).

Compared to the unmodified 6FDA-DAM:DABA (3:2), higher acid gas selectivity and membrane stability are achieved under harsh feed conditions. For pure H_2S, the un-crosslinked 6FDA-DAM:DABA (3:2) showed a plasticization pressure of approximately 2 bar, and as the crosslinker size increased from DEG, TEG, to TetraEG, the plasticization pressure gradually increased from 6 to 8 bar. The plasticization caused by pure CO_2 only occurs when the feed pressure is greater than 25 bar. The crosslinked membranes showed good mixed-gas separation properties, under a mixture of $H_2S/CO_2/CH_4$ (20/20/60) at 62 bar, the selectivity of TetraEG crosslinked membrane exhibited H_2S/CH_4 and CO_2/CH_4 selectivities of 21 and 29 (Fig. 7, Table 4), respectively. This combination of results showed very promising in real highly sour gas removal in NG sweetening,

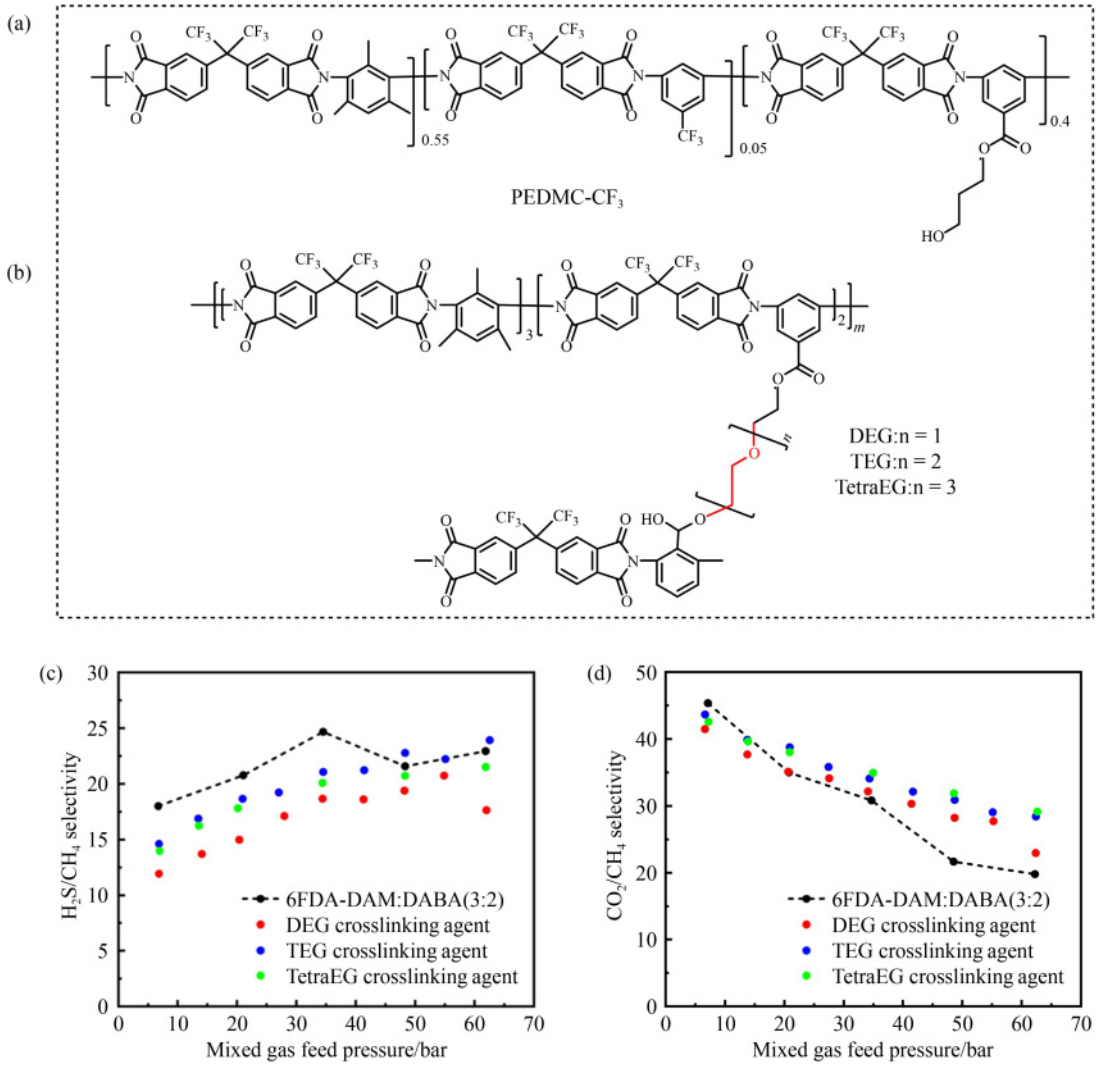

Fig. 7 (a, b) Structure of PEDMC and their ethylene glycol crosslinked with different lengths of EG repeat unit. (c) H_2S/CH_4 and (d) CO_2/CH_4 selectivity of pristine, DEG, TEG, and TetraEG crosslinked 6FDA-DAM:DABA (3:2) under mixed-gas of $H_2S/CO_2/CH_4$ (20/20/60) up to 62 bar feed pressure. Reprinted with permission from Ref. [87], copyright 2013, American Chemical Society.

indicating that crosslinking is an efficient way to enhance the membranes for NG sweetening under harsh conditions.

The CO_2, H_2S permeability and H_2S/CH_4, CO_2/CH_4 selectivity of recently reported PIs are summarized in Table 4. It can be observed that most of the PI membranes show H_2S permeability of 3 to 1076 barrer, and the H_2S/CH_4 selectivity of PI ranging from 7 to 49. Notably, the permeability and selectivity of the H_2S/CH_4 can be improved at the same time by careful molecular design. Additionally, as the feed pressure and H_2S concentration increase, there is also an enhanced H_2S permeability combined with H_2S/CH_4 selectivity increase. This anti-trade-off effect gives PI membranes a great opportunity for H_2S removal from NG at high pressure feed gas mixtures.

3.1.4 PIMs and modified PIMs for H_2S and CO_2 separation

PIMs are a class of polymers characterized by high rigidity and microporosity [88–91]. PIMs have been extensively studied in the field of O_2/N_2 and CO_2/CH_4 separation membranes due to their high free volume and good processability, very high permeability with 2 orders of magnitude than conventional polymers and modest gas pair selectivity [92–95], however, in the field of H_2S/CH_4 separation, due to the lack of interaction between polymer chains, most PIM membranes exhibit low H_2S/CH_4 selectivity in high-pressure gas mixtures, and the structures of some reported PIMs investigated for H_2S separation are shown in Fig. 8.

The poly(1-trimethylsilyl-1-propyne) (PTMSP) is the

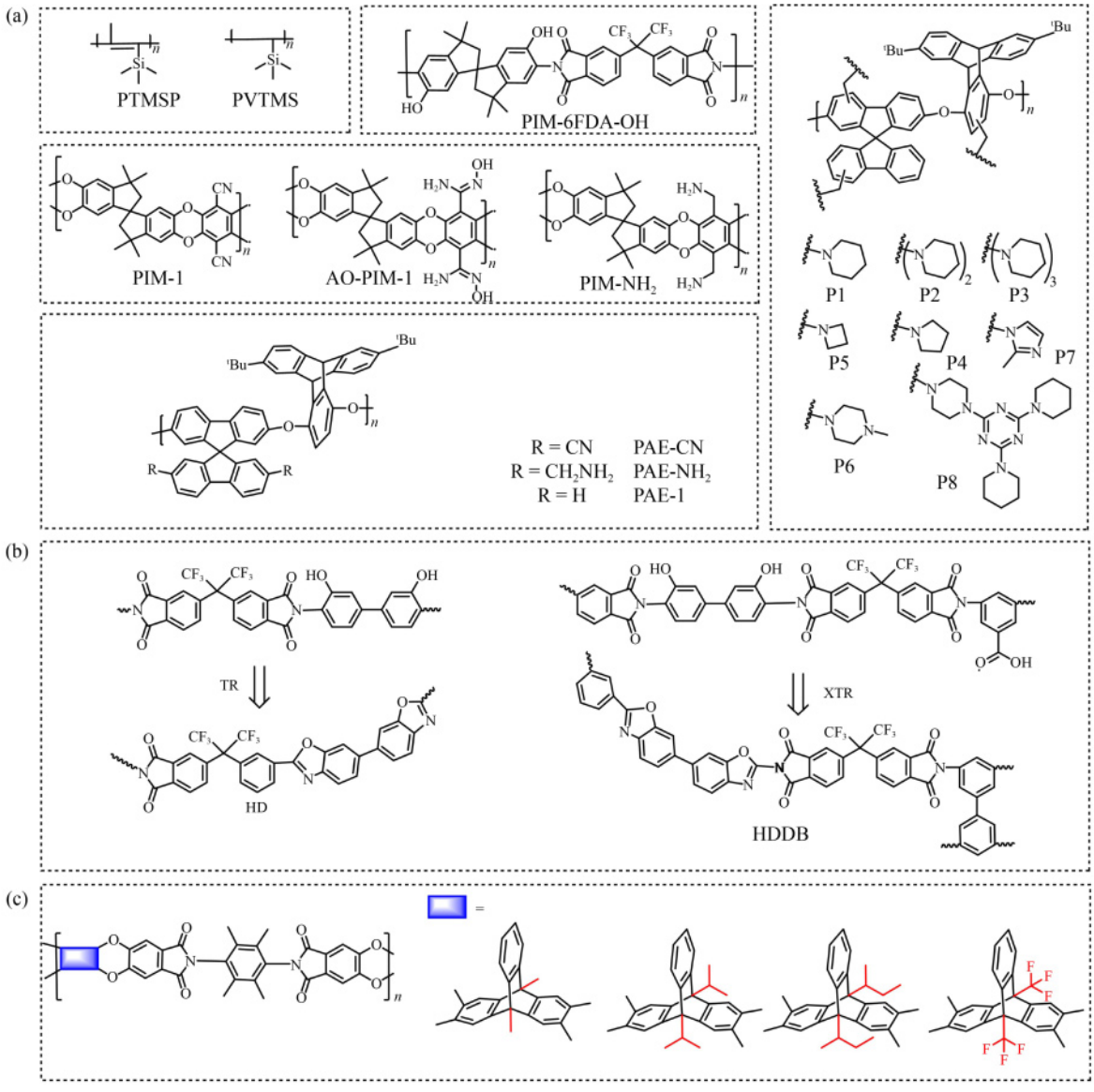

Fig. 8 (a) Structure of PIM and modified PIMs for NG sweetening. (b) Structure and thermally rearranged (TR) process of non-cross-linked TR membrane (HD) and cross-linked TR membranes (HDDB). (c) Simulated structure of triptycene-based PIM-PIs for sour gas removal.

first generation of highly microporous polymer, which was synthesized by Masudu et al. [96] in the 1980s. Merkel tested the temperature dependent H_2S permeability of PTMSP, which demonstrated exceptional H_2S permeability up to 21400 barrer at the pressure of 20 bar [97]. The H_2S permeability of PVTMS was 350 barrer evaluated by Malykh et al. [98] However, its H_2S/CH_4 selectivity is merely 1.6. Although these polymers showed high H_2S permeability, their H_2S/CH_4 selectivity still needs to be improved. In 2015, Yi et al. [99] reported a hydroxy-functionalized PIM PI (PIM-6FDA-OH) with inherent micropores, which showed slight plasticization up to 8 bar of pure H_2S feed. The PIM-6FDA-OH showed significant resistance to pure gas CO_2 plasticization at feed pressures up to 28 bar. In the ternary mixed-gas ($H_2S/CO_2/CH_4$ = 15/15/70) system, with the increase of feed pressure from 6.9 to 48.3 bar, the permeability of H_2S rapidly increased to 63.5 barrer (Table 5), but the permeability of CO_2 decreased to 52.6 barrer due to the higher competitive sorption of H_2S than CO_2, whereas the permeability of CH_4 remained at ~1.9–2.1 barrer, and the H_2S/CH_4 separation factor quickly increased to 29.9. Later, Yi et al. [40] reported an amidoxime functionalized PIM-1 (AO-PIM-1, Fig. 8(a)) as membranes for H_2S separation, which has a larger Brunauer-Emmett-Teller surface area than PIM-6FDA-OH. A ternary feed mixture of $H_2S/CO_2/CH_4$ (20/20/60) was used as feed gas from low pressure up to 77 bar. The AO-PIM-1 membrane showed an unprecedented H_2S permeability of over 4000 barrer and H_2S/CH_4 selectivity of up to 75, this figure-of-merit is among the highest H_2S/CH_4 separation membranes, which is more than one order of magnitude higher in H_2S permeability, and its H_2S/CH_4 selectivity is much higher than those of PI and conventional polymer membranes. The overall H_2S/CH_4 separation, CAG removal performances of the AO-PIM-1 and PIM-1 membranes are shown in the following Figs. 9(a)–9(d). The pristine PIM-1 also showed an H_2S permeability

Table 5 H_2S/CH_4 and CO_2/CH_4 separation properties of PIM and modified PIM membranes

Polymer	$P^{a)}$	$H_2S/CO_2/CH_4$	P_{H_2S} b)	P_{CO_2} b)	P_{CO_2}/P_{CH_4}	P_{H_2S}/P_{CH_4}	Ref.
PTMSP	290	$H_2/CO/CO_2/H_2S$	21400	18200			[97]
PVTMS			350	1600	7.3	1.6	[98]
PIM-6FDA-OH	500	15/15/70	36	55	28	18	[99]
	700	15/15/70	63.5	52.6	25	29.9	
AO-PIM-1 (fresh)	1122	20/20/60	4375	796	13	74	[40]
PIM-1	1122	20/20/60	13800	4850	9	26	
AO-PIM-1 (rejuvenated)	1122	20/20/60	4050	796	12	60	
$PIM-NH_2$	116	13.3/26.7/60	71	103	26	18	[100]
PAE-CN	116	13.3/26.7/60	270	231	13	15	

a) Feeding pressure of the upstream gas; b) permeability of the membranes, unit, barrer.

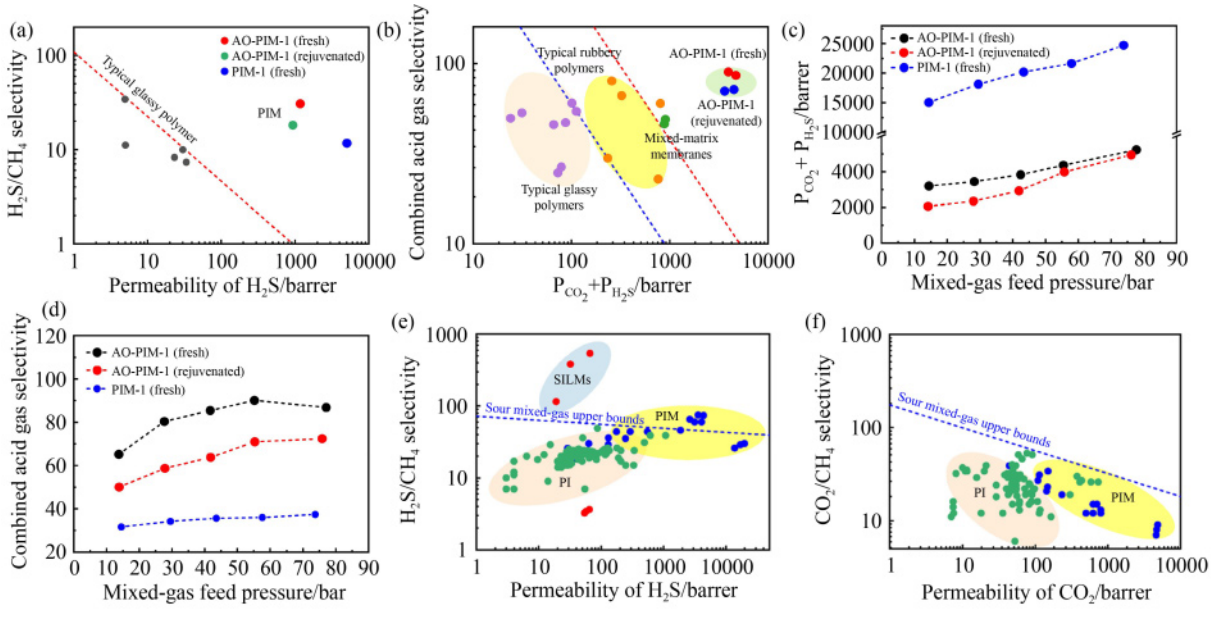

Fig. 9 (a) H_2S/CH_4 and (b) CO_2/CH_4 separation properties of different membranes. (c) Pure-gas (CO_2 + H_2S)/CH_4 separation performance of PIM-1, AO-PIM-1, and some reported polymer membrane. (c, d) CAG separation performance of PIM-1, AO-PIM-1, and some reported glassy and rubber polymers in $H_2S/CO_2/CH_4$ (20/20/60) mixed-gas system at aggressive feed pressures up to 77 bar. Reprinted with permission from Ref. [40], copyright 2019, American Association for the Advancement of Science.

increase with increasing feed pressure, when the upstream pressure went up to 77 bar, the H_2S permeability of PIM-1 reached over 13800 barrer and an H_2S/CH_4 selectivity of 26 (Table 5).

Aside from amidoxime group, the amine based microporous polymers have great potential in H_2S separation applications. Mizrahi Rodriguez et al. [100] and Dean et al. [101] studied the effects of amine-functionalized PIM-1 (PIM-NH_2) and microporous polyaryl ether (PAE-NH_2) on polymer packaging structure and specific transport behavior of CO_2 and H_2S through mixed gas adsorption tests (Fig. 8(a)). It was found that adding primary amine to the microporous polymer could improve the mixed gas separation performance through competition. For example, compared with the nitrile functionalized PAE-CN, the pure gas adsorption rate for PAE-NH_2 was 69% higher for CO_2 and 26% for H_2S at 1.013×10^5 Pa and 35 °C, indicating an increased affinity for both CO_2 and H_2S after amine functionalization. The mixed-gas sorption analysis results indicated that the PIM-NH_2 and PAE-NH_2 showed a much higher solubility selectivity of CO_2/CH_4 and H_2S/CH_4 than their pristine PIM-1 and PAE-CN, indicating the amine functionalized microporous membranes have great potential in the future acid gas removal from NG. Dean et al. [102] circumvent these manufacturing constraints while maintaining competitive-sorption enhancements by synthesizing eight representative microporous PAEs with tertiary amines.

The overall H_2S/CH_4 separation properties and CAG separation performances of PIs and some reported glassy polymers are listed in the following Figs. 9(e) and 9(f). Till now, the amidoxime-functionalized PIM membranes show the most promising H_2S/CH_4 separation, combined $(H_2S + CO_2)/CH_4$ separation performance, with an H_2S permeability of 4000 barrer and an H_2S/CH_4 selectivity of over 70 (Table 5), which is even higher than the 2021 H_2S/CH_4 upper bound.

TR polymer membranes are also another type of highly porous polymer membranes, which were reported by Lee et al. [103] in 2007, who thermally treated a PI with a –OH or –SH group in the ortho position of imide bond at 450 °C, the PI changed to polybenzoxazole (PBO). These PBO membranes significantly improved the permeability and selectivity [28,104−110]. Scholes et al. [111] reported the HD and HDDB series of PI precursors and thermally treated them at 400 °C for 1 h. The membranes were tested at a pressure of up to 1 bar. For cross-linked TR (XTR) membranes (HDDB), their H_2S permeability was observed to decrease with increasing partial pressure, while for the non-cross-linked TR membrane (HD), a constant H_2S permeability with pressure increased was observed (Fig. 8(b)). This is attributed to the permeability within the XTR membrane being H_2S solubility dominated, while in the non-crosslinked TR membrane, permeability was H_2S diffusivity dominated.

Quantum mechanics and simulation techniques to analyze the properties of polymer membranes at the atomic scale are of great significance for understanding the behavior of side groups in gas separation. Ghasemnejad-Afshar et al. [112] used ab-initio calculation, molecular dynamics, and Monte Carlo simulation techniques to study the structural properties of triptycene-based microporous PI with different side groups (C_4H_9, C_3H_7, CH_3, and CF_3) shown in Fig. 8(c). It is found that PIM membranes with larger side groups are more rigid, and the free volume in the polymer chain structure increases, which is conducive to the diffusion and penetration of gases. In particular, membranes with C_4H_9 side groups showed the highest selectivity of all the binary gas mixtures studied. For the binary mixture of CO_2/CH_4 and H_2S/CH_4, the membrane with the CF_3 group (PIM-CF_3) is more selective than PIM-C_3H_7. Although there are some deviations between the permeability and selectivity of the simulation and the experimental results, these simulation results provide useful guidance for synthesis and modification.

3.1.5 Other glassy polymers for H_2S and CO_2 separation

Novel glassy polymer membranes are always desirable in searching for advanced membranes for acid gas removal from NG. Recently, H_2S and CO_2 separation properties of some polyoxadiazole-based polymer derivatives have also been studied by Hayek et al. [113], who synthesized a series of polyazole-based polymer membranes (POz-CF_3 and FPT-Ph(OH)) for H_2S separation with their structures shown in Fig. 10(a).

Both membranes showed good plasticization resistance up to 700 psi. The FPT-Ph(OH) exhibited a very high H_2S permeability of 119 barrer and H_2S/CH_4 selectivity of 21.4. This figure-of-merit is significantly higher than that of conventional PIs. Meanwhile, the two polymer membranes showed a big difference in both permeability and selectivity. Specifically, the FPT-Ph(OH) membrane not only showed 2 and 3 times higher CO_2 and H_2S permeability than POz-CF_3, but also 1.6- and 4.1-fold higher CO_2/CH_4 and H_2S/CH_4 selectivity (Table 6). This can be ascribed to the H_2S-induced plasticization that hugely improved the permeability of H_2S in FPT-Ph(OH) membranes, but the enhancement in selectivity still needs to be analyzed in detail.

Lawrence et al. [114] investigated the performance of alkoxysilane-substituted VAPNBs for CO_2 and H_2S separation from NG (Fig. 10(b)). They studied the acid gas separation performances of 10 different VAPNBs were studied by varying the alkoxysilane-substituted groups. Most of these membranes showed extremely high CO_2 and H_2S permeability ranging from 1000 to 4200 barrer combined with relatively high CO_2/CH_4 and H_2S/CH_4 selectivity. Among them, the P7 with 2-methoxy-ethoxy-silicyl group exhibited an H_2S

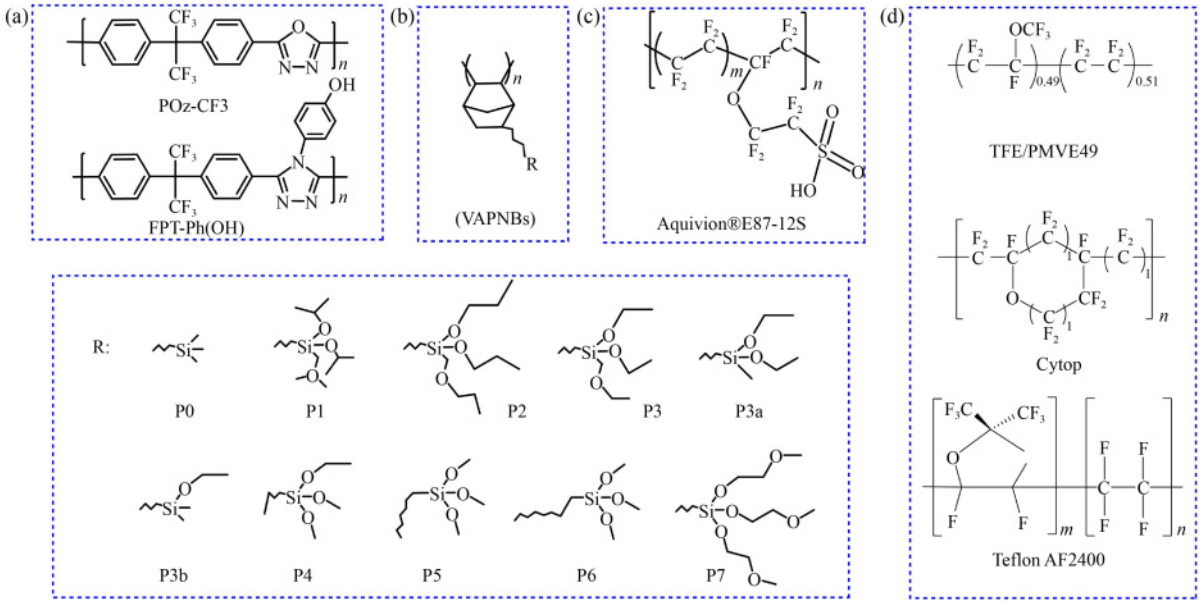

Fig. 10 Chemical structure of the (a) POz-based polymers, (b) vinyl-added polynorbornene (VAPNB) series, (c) Aquivion®E87-12S, and (d) some perfluorinated polymers.

Table 6 Permeability and selectivity of some unconventional glassy polymers for acid gas removal from NG

Membrane	$P^{a)}$	$H_2S/CO_2/CH_4$	P_{H_2S} b)	P_{CO_2} b)	P_{CO_2}/P_{CH_4}	P_{H_2S}/P_{CH_4}	Ref.
POz-CF_3	500	20/10/59	41.0	43.1	5.06	5.32	[112]
POz-CF_3	700	20/10/59	38.8	40.6	5.20	5.49	
FPT-Ph(OH)	500	20/10/59	136	92.0	22.0	14.9	
FPT-Ph(OH)	700	20/10/59	119	79.8	21.4	14.3	
P0	800	5/3/92	4186	2736	6.5	4.27	[113]
P1	800	5/3/92	3170	1373	8.2	3.62	
TEE/PMVE/8CNVE	100	$H_2S/CO_2/CO/H_2$ (0.7/11.7/36.5/51.1)	3.50	28	–	–	[114]
Teflon AF 1600	20	$H_2S/CO_2/CO/H_2$ (1.5/10.5/46/42)	100	680	–	–	
Teflon AF 2400	20	$H_2S/CO_2/CO/H_2$ (1.5/10.5/46/42)	410	2300	–	–	
Cytop	100	$H_2S/CO_2/CO/H_2$ (0.7/11.7/36.5/51.1)	0.63	17	–	–	
Perfluorosulfonic acid (PFSA)	43.5	$H_2S/CO_2/CH_4$ (9/10/81) RH (relative humidity) = 20%, T = 25 °C	30.9	45.8	19.7	29.2	[115]
	43.5	RH = 50%, T = 25 °C	145	126	45.3	39.2	
	43.5	RH = 80%, T = 50 °C	480	445	20.2	18.8	

a) Feeding pressure of the upstream gas, psi; b) permeability of the membranes, unit, barrer.

permeability of up to 3130 barrer, and H_2S/CH_4 selectivity of 47.8 (Table 6). VAPNBs have demonstrated excellent performance in acid gas separation, making them one of the most promising materials in the field of H_2S removal from NG.

Perfluorinated polymers are very promising candidates due to their exceptional thermal and chemical stability. They can be dissolved only in certain perfluorinated solvents to fabricate into thin-film composite membranes. The perfluorinated polymers demonstrate lower solubility coefficients for both CO_2 and H_2S than those conventional hydrocarbon polymers, and thus, they show much higher CO_2/H_2S solubility selectivity. The Teflon AF 2400 and Teflon AF 1600 showed very high H_2S permeability of 410 and 100 barrer, respectively. Merkel and Toy [115] found out that both Cytop and Teflon on membranes were capable of absorbing more CO_2 than H_2S, resulting in much higher CO_2/H_2S solubility selectivity ~1.2 to 1.5. They also point out that fluorinated polymers are more plasticization-resistant as compared to non-fluorinated polymers as they are highly resistant to chemical degradation which allows them to withstand acidic conditions without a decrease in performance.

Humidified H_2S and CO_2 separation performances were also studied by a PFSA (Aquivion® E87-12S) membrane with the mixed-gas of $H_2S/CO_2/CH_4$ (9/10/81) at 50 °C and upstream pressures up to 10 bar, and the RH changes from 20% to 90% (Fig. 10(c)) [116]. The results showed that there is a strong dependence of PFSA separation performance on water activity and temperature (Fig. 10(d)). There is a sharp increment in H_2S permeability as the temperature and RH increase, for example, the H_2S permeability reaches 500 barrer at 50 °C and

80% RH. Notably, the CO_2, CH_4 and H_2S permeability enhancement by the humidity for Aquivion® E87-12S is much larger than the temperatures and upstream pressures parameters. Moreover, under the humidified conditions, both CO_2 and H_2S simultaneously enhanced sharply but the CO_2/CH_4 and H_2S/CH_4 selectivity are almost kept constant, which hugely improves its acid gas removal ability.

3.2 Rubber polymers for H_2S and CO_2 separation

Rubber polymers are a type of polymers with their glassy transition temperatures below room temperature. Rubber polymers are widely applied for H_2S separation, because the rubber polymers have very high solubility selectivity for H_2S/CH_4, which always results in pretty high H_2S/CH_4 selectivity. Recently, most of the rubber polymers used in sour gas removal are generally composed of a soft part and a hard segment to keep the shape of the membrane whereas maintain its flexibility.

Polyurethane is a typical rubber polymer that contains –NHCOO– groups that are synthesized by the reaction of isocyanate with aliphatic or aromatic di-alcohols, and widely used in furniture, bedding, and seating, thermal insulation, elastomers and coatings due to its flexible, durable and adjustable properties. Chatterjee et al. [56] synthesized two polyether urethane (PU1 and PU3) and two PU urea (PU2 and PU4) membranes

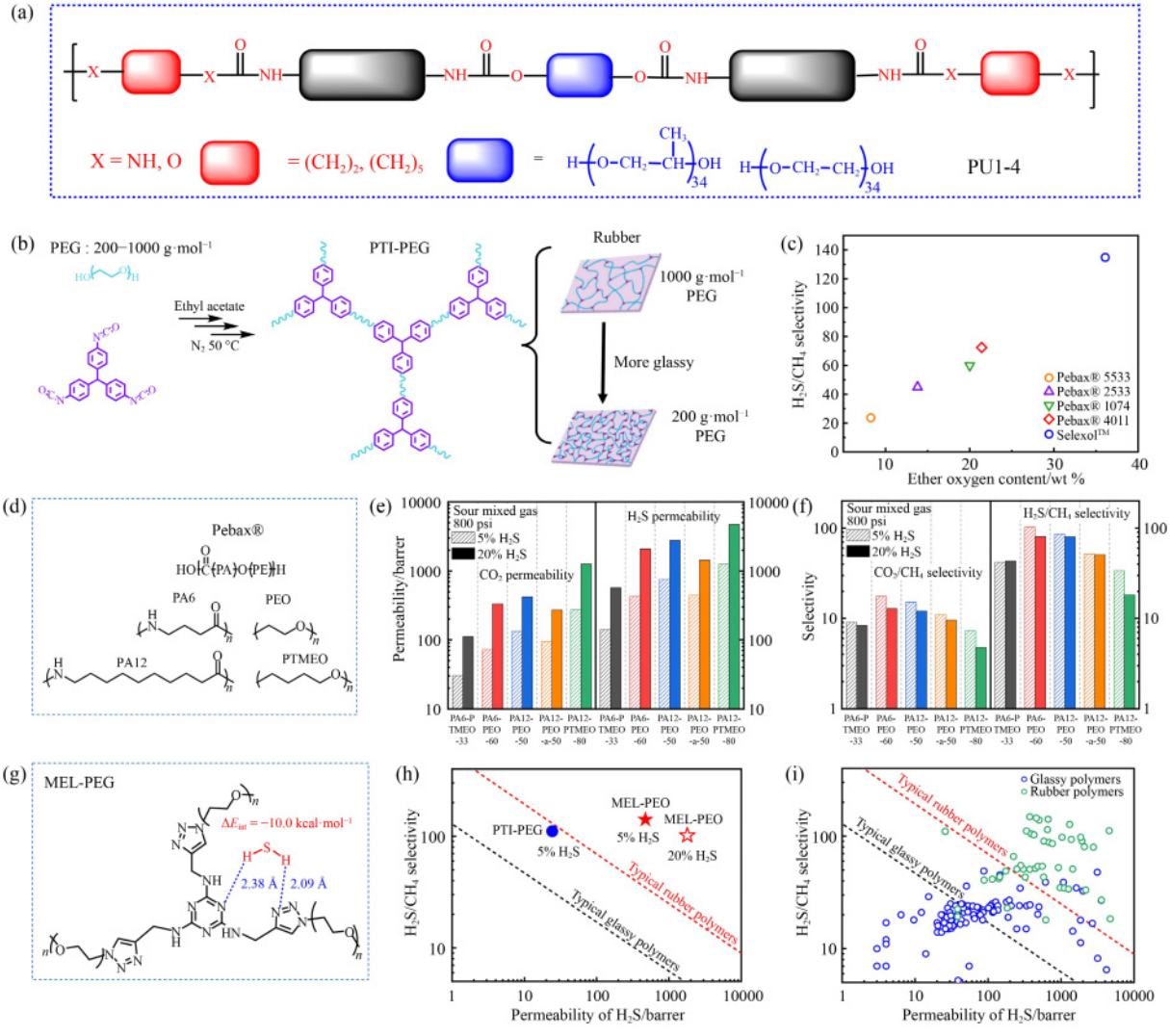

Fig. 11 (a) Structures of the PU and PU urea and their building blocks from PU1-4. (b) Crosslinked PU membranes using the length of PEG to adjust the crosslinking node concentration. Reprinted with permission from Ref. [119], copyright 2020, Elsevier. (c) The correlation of H_2S/CH_4 selectivity and the ether oxygen content for Pebax. (d) The chemical structure of Pebax, the polyamide (PA) part and PE part are highlighted. (e) The CO_2 and H_2S permeability as the structure and H_2S concentration change. (f) The CO_2/CH_4 and H_2S/CH_4 selectivity as the structure and H_2S concentration change. Reprinted with permission from Ref. [120], copyright 2022, Elsevier. (g) Structure of MEL-PEG, and (h) its performance on the trade-off lines, the binding energy between H_2S and MEL-PEG. Reprinted with permission from Ref. [121], copyright 2024, Elsevier. (i) H_2S-separation performance of glassy and rubber polymer membranes.

Table 7 Summary of H_2S/CH_4 and CO_2/CH_4 separation properties for rubber polymers

Membrane	$P^{a)}$	$H_2S/CO_2/CH_4/N_2/C_2H_6$	P_{H_2S} b)	P_{CO_2} b)	P_{H_2S}/P_{CH4}	P_{CO_2}/P_{CH_4}	Ref.
PEI-PEG1000	55.2	5/3/92	25.9	5.2	110	22.1	[119]
PEI-PEG300	55.2	5/3/92	0.24	0.11	38.4	81.3	
Pebax® 1657	55.2	5/3/92	426	72.3	103	17.5	
Pebax® 2533	55.2	5/3/92	1260	273	33.9	7.3	
PA12-PEO-50	200	5/3/92	581	97.8	90.4	15.2	[120]
	500	5/3/92	684	117	88.1	15.0	
	800	5/3/92	760	133	86.0	15.1	
PA6-PEO-60	200	5/3/92	336	52.3	111	17.4	
	500	5/3/92	390	65.7	105	17.7	
	800	5/3/92	426	72.3	103	17.6	
Pebax/EOA-100	72.5	3/3/94	4564	303	111.9	7.43	[122]
PPG-HDI-BOO	145	0.66% H_2S	790	473	27.2	16.3	[117]
PU1	145	12.5/18.1/69.4	183	55.8	23	7.01	[56]
PU4 (35 °C)	145	1.3/27.9/70.8	199	44.7	74	17	
PU4 (20 °C)	145	1.3/27.9/70.8	102	22.4	102	22	
Pebax MX 1074	145	12.5/18.1/69.4	553	122	54	11.9	
Pebax MX 1657	145	12.5/18.1/69.4	248	69.1	51	14.2	
Pebax MX 1041	145	12.5/18.1/69.4	175	39.7	49	11.1	
MEL-PEG_{1100}	800	5/3/92	501	79	139	21.8	[121]
	800	20/10/57/10/3	1860	264	97.9	13.9	

a) Feeding pressure of the upstream gas, psi; b) permeability of the membranes, unit, barrer.

by adjusting the polyether (PE) and 1,5-heptanyl-diol or 1,5-heptanyl-diamine linkages for H_2S separation from "low-quality" NG (Fig. 11(a)). The results demonstrated that the PU4 membrane exhibited an H_2S/CH_4 selectivity of 76 at 35 °C and over 100 at 20 °C and 10 bar under mixed gas $H_2S/CO_2/CH_4$ (70.8/27.9/1.3) (Table 7), which is one of the highest values reported at the time, and the higher H_2S/CH_4 selectivity of PU4 than PU3 is probably due to the more polar of urethane urea group. When the H_2S concentration increased from 1.3% to 12.5%, the H_2S/CH_4 selectivity decreased from 102 to 95 (Table 6), which is most probably due to the competitive sorption of H_2S.

Sadeghi et al. [117] introduced a novel PU (polypropylene glycol-hexamethylene diisocyanate-1, 4-butane diol, PPG-HDI-BDO) membrane that synthesized from PPG, HDI, and BDO, which showed a very high H_2S permeability of 790 barrer, and H_2S/CH_4 selectivity of 27.2 for ternary $CH_4/CO_2/H_2S$ (H_2S% of 0.66%) gas mixtures, respectively. This result is the highest among the reported PU membranes. Meanwhile, it also showed a CO_2 permeability is 473 barrer combined with CO_2/CH_4 selectivity of 16.3. This study also revealed that as operating pressure and temperature increased, both the permeability and selectivity for H_2S and CO_2 improved. These figure-of-merits confirmed the excellent CAG removal ability for this PPG-HDI-BDO. Mohammadi et al. [118] investigated the permeation behavior of H_2S, CO_2, and CH_4 through poly (ester urethane urea) (PEUU) membranes under varying operational conditions. As pressure increased, the permeability of H_2S and CO_2 decreased, which is likely due to the compressive effects on the membrane. However, higher temperatures significantly enhanced gas permeability, indicating that the permeation behavior was primarily diffusion-controlled. Although the membrane performed excellent H_2S separation properties, its selectivity was slightly inferior to that of Pebax® and PEO-based membranes.

Harrigan et al. [119] reported a novel type of crosslinked PU (PTI-PEG) by reacting the methylidyne tri-*p*-phenylene triisocyanate and PEG. The H_2S/CH_4 and CO_2/CH_4 separation performance of the PEI-PEG membrane can be adjusted by the crosslinking density by adjusting the molecular weight of PEG (200 *vs.* 1000) (Fig. 11(b)). The findings revealed that by crosslinking PEG of varying molecular weights, membranes made from low-molecular-weight PEG were more suited for CO_2/CH_4 separation, whereas those made from high-molecular-weight PEG performed better in H_2S/CH_4 separation. The small molecular weight PEG induced a high crosslinking density, which makes the membrane more like a glassy polymer. However, with high PEG molecular weight, the crosslinking density is reduced, and more rubber effects on the H_2S/CH_4 separation properties are observed.

Pebax® is a thermoplastic elastomer developed by Arkema Group, and frequently utilized in the preparation of gas separation membranes. It is composed of block copolymers of PE and PA, where the PE segment provides flexibility, elasticity, and high gas permeability, while the PA segments provide mechanical strength and chemical resistance (Fig. 11(c)). An examination of the ether-associated oxygen content in the various Pebax membranes were reported by Kraftschik et al. [42] and shown in Fig. 11(d), the almost linear regression curve indicates that a strong correlation between the ether

content in the Pebax with H_2S/CH_4 selectivity exists. Harrigan et al. [120] investigated the transport properties of various Pebax® membranes in high-pressure NG separation, focusing on acidic gases such as H_2S and CO_2. The results demonstrated that Pebax® 1074 and 1657 membranes, which contain 50% and 60% PEO, respectively, exhibited H_2S/CH_4 selectivity of 79.9 and 80.6, and CO_2/CH_4 selectivity of 12.0 and 12.8, under a high-pressure mixed gas environment containing 20% H_2S (Table 7). As pressure increased, the CO_2/CH_4 selectivity of all membranes decreased by an average of 24%–42% (Figs. 11(e) and 11(f)), with a more pronounced effect in high H_2S environments. The study indicated that membrane stability was linked to hydrogen bonding, with PEO-containing membranes demonstrating enhanced anti-plasticization properties due to stronger hydrogen bonding interactions. This research underscores the importance of testing membrane materials under realistic gas conditions, highlighting the potential of Pebax® membranes for NG treatment in environments with elevated H_2S concentrations.

PEG materials exhibit flexibility and tunable physical properties in the separation of acid gases. Wong et al. designed a series of melamine-crosslinked PEG membranes (Figs. 11(g) and 11(h)), synthesized via azide-alkyne cycloaddition (click chemistry), for the efficient separation of acid gases (H_2S and CO_2) [121]. The resulting membrane exhibited exceptional permeability and selectivity for H_2S and CO_2 under high pressure conditions (55 bar), particularly in acid gas removal and enrichment processes. The study also found that the molecular weight of the PEG chains had a significant impact on membrane performance, with high-molecular-weight PEG (such as PEG 1100) exhibiting superior selectivity and permeability for H_2S/CO_2 separation, which is consistent with the findings of Harrigan et al. [119].

Vaughn and Koros [74] conducted a comparative analysis of the acid gas separation performance of the glassy polymer 6F-PAI-1 and the rubbery polymer Pebax® in NG purification. The results showed that 6F-PAI-1 achieved a CO_2/CH_4 selectivity of 40 and an H_2S/CH_4 selectivity of 20. Notably, the selectivity of Pebax® remained largely unaffected by variations in acid gas concentrations, which is consistent with the behavior of rubbery materials. The superior anti-plasticization performance of 6F-PAI-1, particularly under high CO_2 concentrations, makes it highly suitable for maintaining stable separation performance in complex environments.

Compared with the high H_2S selective rubber material, which shows a higher H_2S separation ability (Fig. 11(i)). However, the glassy PI membranes have much higher CO_2/CH_4 selectivity, which will benefit the reduction of CH_4 loss in the downstream. Therefore, under the low H_2S feed condition, the glassy polymer with higher CO_2 selectivity is more suitable, while at the high H_2S content, the rubber polymer is preferred to deacidification for NG separation. On the other hand, glassy PI membranes also have a plasticization benefit in high-pressure of H_2S/CH_4 separation, which will also facilitate their H_2S removal performance.

3.3 CMSMs for H_2S and CO_2 separation

The CMSMs possess extreme rigidity, separation performances for conventional gas pairs, and utmost thermal and chemical stabilities [123−129]. However, these membranes for H_2S separations are quite limited. Tronci et al. [130] theoretically analyzed gas transport through nanoporous graphite membranes for NG purification. And the results indicated that the pore size, shape, and functionalization of graphene severely affect the selectivity of the membrane toward CO_2/CH_4 and H_2S/CH_4 gas pairs. Four different pore structures and functionality are used as model compounds for simulating the H_2S, CO_2, and CH_4 transport, and their pore structures as well as the three-dimensional structures of the molecules are shown in the following Fig. 12. The results indicated that the P1 showed the best H_2S/CH_4 selectivity of 20 combined with a pretty high CO_2/CH_4 selectivity. This result suggests that the circular pore for the separation of H_2S and CO_2 from CH_4 with graphene membranes is 5.90 Å.

Haider et al. [131] analyzed the CTA derived carbon molecular sieve hollow fiber membranes (CHF) for long-term acid gas removal from NG. Different storage

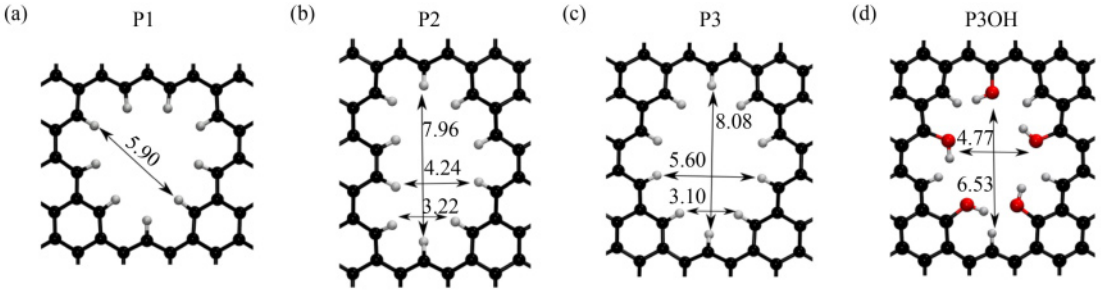

Fig. 12 Ball and stick representation of the porous graphene structures employed for gas separation (zoomed on the pore area). Carbon atoms are represented in black, oxygens in red and hydrogens in white. Distances are in Angstrom. Reprinted from Ref. [130].

conditions were carried out to evaluate the long-term permeability stability. When the CHF was exposed to high (150 to 2400 ppm) H_2S conditions, the resulting CHF showed an improved CO_2 permeability but decreased CH_4 permeability after storage for the first 30 d. However, after 4 months, the CO_2 permeability decreased by almost 70%, which is due to the pore blockage of H_2S.

4 Hollow fiber and thin film composite (TFC) membranes for H_2S and CO_2 separation

4.1 CA hollow fiber membrane for H_2S separation

Hollow fiber membrane is a fiber-like membrane with self-supporting structure, ultra-thin circulated skin layer, and porous supported layer, excellent surface area/volume ratio due to its high packing density is widely applied for real gas separation applications [132]. The application of polymeric membranes for NG deacidification has been widely investigated for a long time, in which, CA membranes due to their partially crystallized and robust that can withstand extremely high pressure and some associated components in the NG. Up to now, CA hollow fiber membrane is still the major membrane for acid gas removal in industries. Some representative products are listed in Cynara (Fig. 13), in which, the single Cynara CA membrane module can reach as much as 30 inches in diameter with a weight of 3.5 t.

Morisato and Mahley et al. [133] reported the effect of feed pressure and temperature on the separation performance of asymmetric CTA hollow fiber membranes. The permeance of CTA hollow fiber membrane increased with the increase of feed pressure, and the selectivity of H_2S/CH_4 was basically stable at low pressure, while it declined sharply when the pressure was above 30 bar. The mixed gas permeability of H_2S and CO_2 increased with the decrease in feed temperature. The CTA hollow fiber membrane showed the best performance at 15 °C and 39 bar, the permeability of H_2S

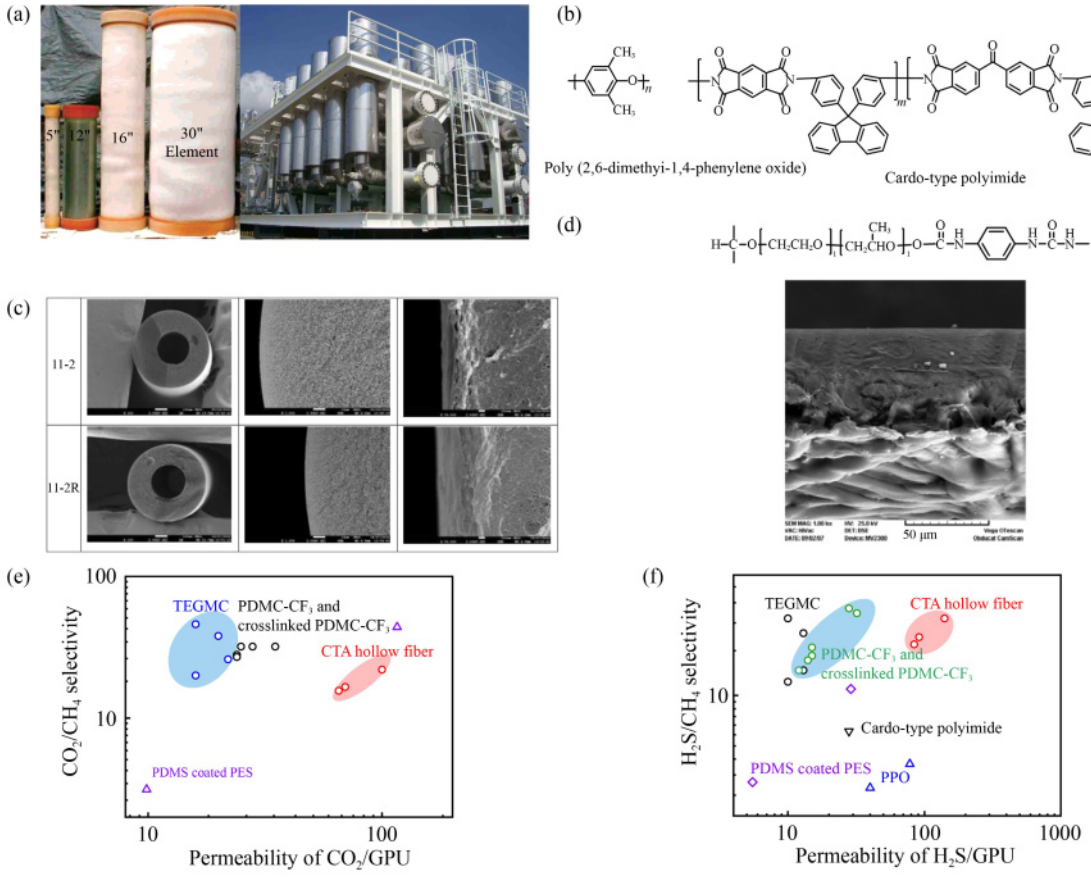

Fig. 13 (a) CTA hollow fiber membrane module with 30-inch size and arrays of CTA hollow fiber module for NG sweetening in Cynara. Reprinted with permission from Ref. [5], copyright 2008, American Chemical Society. (b) The cross-sectional image of CTA hollow fiber membranes of 11-2 and 11-2R. Reprinted with permission from Ref. [58], copyright 2024, Elsevier. (c) Chemical structure of commercial PPO (supplied by Aquilo Gas Separation B.V., the Netherlands) and Cardo-type PI (supplied by RITE, Japan). (d) The structure of PEUU and the SEM image of the composite membrane. Reprinted with permission from Ref. [118], copyright 2008, American Chemical Society. (e, f) The permeance of CO_2 and H_2S as well as the CO_2/CH_4 and H_2S/CH_4 selectivity for hollow fiber membranes.

and CO_2 were 180 and 133 GPU, and the selectivity of H_2S/CH_4 and CO_2/CH_4 was 23 and 16, respectively. CTA hollow fiber membranes also showed good performance for H_2S separation under practical application conditions, with excellent H_2S high pressure and temperature tolerance.

Peters et al. [58] used a dry-wet spinning method to make the CA hollow fiber membrane using the component ratio and spin conditions (Table 8). The resulting CA hollow fiber membrane showed a dense spongelike cross-section image (Fig. 13(b)), which has a H_2S permeance of 84 GPU and H_2S/CH_4 selectivity of 19.8 under 15% H_2S in the feed condition at 20 bar and the stage-cut of 5% (Table 9). When the stage cut decreased to 1%, both H_2S permeance and H_2S/CH_4 selectivity increased to 91.3 and 21.8. Notably, the results also confirmed that there is almost no change of H_2S permeance as well as H_2S/CH_4 selectivity under humidified feed gas, with H_2S permeance of ~80 GPU and H_2S/CH_4 selectivity of 23 at 1.5% stage-cut under humidified gas condition.

Lu et al. find that the plasticization for CTA hollow fiber membrane can be benefit for H_2S/CH_4 separation in raw NG sweetening [134]. The separation performance of CTA hollow fiber membrane was tested in NG mixtures containing high concentrations of H_2S, CO_2, C_2H_6, C_3H_8, and trace amounts of toluene. When the upstream pressure increased from 7 to 31.3 bar, the CTA hollow fiber membrane exhibited an H_2S permeance increased from 90 to 140 GPU and H_2S/CH_4 selectivity enhanced from 25 to 28 at 35 °C. However, the CO_2 permeance increased from 90 to 115 GPU, whereas the CO_2/CH_4 selectivity decreased from 25 to 22 (Table 10).

Table 8 Dope compositions and conditions of spin trials for CTA hollow fiber membranes

	C-CTA-11-2	C-CTA-11-2R
wt % polymer	22	22
wt % NMP	61	61
wt % acetone	15	15
% LiCl	2	2
Bore fluid wt% (NMP/H_2O)	20/80	20/80
Chimney length/cm	13	13
N_2-flow chimney/(L·min^{-1})	2.5	2.5
Dope flow/(mL·min^{-1})	3.3	3.3
Bore flow/(mL·min^{-1})	0.56	0.56
Pulling speed/(m·min^{-1})	9.6	9.6

4.2 PPO hollow fiber for H_2S and CO_2 separation

The PPO is a linear amorphous thermoplastic with T_g

Table 9 Module C-CTA-11-2R-X, performance at respectively low/high feed flow rate (t = 30 °C and P = 20 bar)

Condition	Flow/stage-cut	T/°C	P/bar	CO_2/GPU	H_2S/GPU	CO_2/CH_4	H_2S/CH_4
5% CO_2	Low/5%	30	20	49.8	–	17.4	–
15% H_2S		30	20	65.3	84	15.6	19.8
5% CO_2	High/1%	30	20	54.2	–	18.7	–
15% H_2S		30	20	69.6	91.3	16.6	21.8

Table 10 The H_2S/CH_4 and CO_2/CH_4 separation performance of hollow fiber on binary or ternary sour NG separation

Polymer	$P^{a)}$	$H_2S/CO_2/CH_4/N_2/C_2H_6$	P_{H_2S} b)	P_{CO_2} b)	P_{H_2S}/P_{CH_4}	P_{CO_2}/P_{CH_4}	Ref.
6FDA-durene/6FDA-CARDO (5000/5000) TFC	350	10/10/59/20/1	223	120	19.3	10.3	[141]
PDMS coated PES	145	0.4/2.1/97.5	28.9	116	10.9	43.9	[137]
PDMS coated PES	435	0.4/2.1/97.5	5.51	9.85	3.14	3.14	
CTA hollow fiber	450	$CH_4/CO_2/H_2S/C_2H_6/C_3H_8$/ Toluene (69/5/20/3/3/300 ppm)	140	100	28	22	[142]
CTA hollow fiber	290	5/15/80, stage cut (5%)	84	65.3	19.8	15.6	[58]
	290	5/15/80, stage cut 1%	91.3	69.6	21.8	16.6	
PPO	100	H_2S/CH_4 (401 ppm H_2S)	78	–	4	–	[136]
Cardo-type polyimide	100	H_2S/CH_4(401 ppm H_2S)	28	–	6.2	–	
TEGMC without PDMS coating	700	5/45/50	10	16	12	20	[139]
TEGMC with PDMS coating	700	5/45/50	10	16	28	46	
TEGMC without PDMS coating	500	20/20/60	13	22	14	26	
TEGMC with PDMS coating	500	20/20/60	13	20	23	38	
Uncrosslinked PDMC-CF_3 hollow fiber	450	0.5/20/79.5	28	28	32	32	[138]
Uncrosslinked PDMC-CF3 hollow fiber	300	20/20/60	15	25	19	32	
Uncrosslinked PDMC-CF_3 hollow fiber	450	25/5/70	15	24	17	27	
Crosslinked PDMC-CF_3 hollow fiber	450	0.5/20/79.5	32	35	30	32	
Crosslinked PDMC-CF_3 hollow fiber	450	20/20/60	14	24	16	28	
Crosslinked PDMC-CF_3 hollow fiber	450	25/5/70	12	24	14	27	

a) Feeding pressure of the upstream gas, unit, psi; b) permeance of the membranes, unit, GPU, 1 GPU = 10^{-6} cm^3·cm^{-2}·s^{-1}·cmHg^{-1}.

~490 K. Because of the phenyl rings, PPO is hydrophobic in nature and has excellent resistance to water, acids, bases, and alcohols. Chenar et al. [136] investigated the H_2S removal from NG in a series of bench-scale experiments using a commercial PPO membrane module (Parker Filtration and Separation B.V., The Netherlands), at the H_2S concentrations ranging from 101 to 401 ppm, with a stage cut of 5%. The H_2S permeance of PPO increases with the feeding pressure of H_2S, from 50 to 100 psi, the H_2S permeance increases from 46 to 64 GPU when the H_2S concentration is 198 ppm. Meanwhile, the higher the H_2S concentration, the larger the H_2S permeance, at the same time, their H_2S/CH_4 selectivity was not affected to be ~4. Furthermore, hollow fiber CTA membranes was also studied at various H_2S concentrations (100–5000 ppm) in CH_4/H_2S binary synthetic gas mixtures and a real NG sample obtained from a gas refinery by Niknejad et al. [135]. When the H_2S concentration increased from 968, 3048 to 5008 ppm in NG. There is a huge increased H_2S permeance of ~2–3 times and good enhancement in CH_4 enrichment was observed. When the H_2S feeding is 3048 ppm, the retentate H_2S decreases to 2033 ppm, whereas the permeate H_2S is 6751 ppm. Notably, when the temperature increased from 293.15 to 313.15 K, there was an increased separation performance of the PPO membrane for H_2S removal. The H_2S concentration of 3048 ppm, the retentate H_2S decreased from 2033 to 1815 ppm.

Chenar et al. [136] compared the performance of commercial PPO (supplied by Aquilo Gas Separation B.V., the Netherlands) and Cardo-type PI (supplied by RITE, Japan) hollow fiber membranes in separating H_2S from CH_4 at different concentrations (structures shown in Fig. 13(c)). As the feed pressure increased from 50 to 100 psi, there is an improvement for H_2S permeance for both PPO (from 60 to 74 GPU) and Cardo-PI (from 15 to 25 GPU) at the H_2S concentration of 198 ppm. In the presence of H_2S the permeance of CH_4 declined for the Cardo type PI membranes, whereas for the PPO membranes it remained relatively unchanged. The H_2S/CH_4 separation factors are ~4 for PPO and ~6 for Cardo-PI hollow fiber membranes and these value increases as the concentration of H_2S increase. Meanwhile, at high operating temperatures, these membrane materials can still maintain their separation properties.

Saedi et al. [137] prepared an asymmetric PES membrane via a phase inversion method and coated it with polydimethylsiloxane (PDMS) for NG decarboxylation and desulfurization. The DMF with the highest solubility parameter give the lowest CO_2 permeance of 4.7 GPU and highest CO_2/CH_4 selectivity of 19 than DMAc and NMP. The H_2S permeance of PDMS coated PSF asymmetric membrane is 32.8 GPU and H_2S/CH_4 selectivity of 11.4, however, both the H_2S permeance and H_2S/CH_4 selectivity decreased sharply as the feed pressure increased.

4.3 PI hollow fiber membrane for H_2S and CO_2 separation

PI hollow fiber membranes are also investigated for H_2S and CO_2 separation applications. Liu et al. [138] made a 6FDA based PI hollow fiber membrane that is semi-rigid, cross-linked, and defect free, aiming to improve the separation efficiency of H_2S and CO_2 in acidic NG. The membrane was evaluated in pure H_2S and three simulated acidic NG environments. The experimental results show that, due to its rigid molecular structure, the subtle asymmetric nanostructure of the membrane is maintained and the H_2S permeability is not decreased during the crosslinking process. In acidic NG environments with low concentrations of H_2S (0.5% H_2S, 20% CO_2, 79.5% CH_4), the crosslinked hollow fiber membrane achieved an H_2S permeance of 32 GPU and H_2S/CH_4 selectivity of 30 at 450 psi and 35 °C. At the same time, the permeance of CO_2 and the selectivity of CO_2/CH_4 are also effectively maintained, with 35 GPU and 32 respectively (Table 10). Under more challenging acidic NG environments (e.g., 25% H_2S, 5% CO_2, 70% CH_4 and 20% H_2S, 20% CO_2, 60% CH_4), un-crosslinked CF_3 hollow fibers showed plasticization. Interestingly, this plasticization is beneficial for H_2S separation, with un-crosslinked samples showing slightly higher H_2S permeance and H_2S/CH_4 selectivity than cross-linked samples. In addition, the effect of acid gas composition on the properties of the membrane was also discussed. The results revealed that the increase of H_2S concentration in acidic NG has a significant effect on the permeability and selectivity of H_2S and CO_2, compared with the increase of CO_2 concentration in feed. Liu et al. [139] also studied the H_2S and CO_2 removal efficiency of triethylene glycol monoesterification crosslinked (TEGMC) hollow fiber membrane under actual NG sweetening conditions (H_2S (25%), CO_2 (5%), CH_4 (64%), C_2H_6 (3%), C_3H_8 (3%) and toluene (100 ppm)). The resulting TEGMC-crosslinkable hollow fiber membranes still show good gas separation properties after 7 years of storage. The permeance for CO_2 and H_2S is ~32, and 10 GPU combined with their CO_2/CH_4 and H_2S/CH_4 selectivity of 55 and 19, respectively. Unexpectedly, the presence of various hydrocarbons in the feedstock gas, namely C_2, C_3, and toluene, increased the selectivity of H_2S/CH_4 and CO_2/CH_4. The author proposed that the infiltration competition may be a useful tool rather than a matter of adjusting membrane properties. Shalabi et al. [140] studied the potential separation performance of 6FDA-durene/6FDA-CARDO (5000:5000) hollow fiber membranes. Preliminary screening studies show good pure gas performance, with a CO_2/CH_4 selectivity coefficient of about 28 and a CO_2 permeance between 310 and 350 GPU. To evaluate the performance of the membrane under simulated industrial environmental conditions, a quaternary gas mixture was tested with feed pressures up to 900 psi and stage cuts from 5 to 20

percent. As the feed pressure increased to 900 psi, the gas mixture permeability and CO_2/CH_4 selectivity of all gases remained relatively stable. The CO_2 permeance and CO_2/CH_4 selectivity of the mixed gas decreased with the increase of stage cut. As expected, due to the trade-off between recovery and purity, as CO_2 recovery is maximized, CO_2 purity is minimized, and CH_4 loss increases with stage cut.

By comparison of the CTA hollow fiber and PI hollow fiber membranes for CO_2 and H_2S removal (Fig. 13), we can clearly conclude that the permeance of CTA is still the best membrane with pretty high CO_2 and H_2S permeance as well as CO_2/CH_4 and H_2S/CH_4 selectivity.

PI is also used for TFC membranes for H_2S separation applications. Yahaya et al. [141] also successfully coated a thin layer of 6FDA-durene/6FDA-CARDO block copolyimide onto a mesoporous polyacrylonitrile acrylate substrate, providing an effective solution for efficient separation of acid gases from NG. The membrane demonstrated excellent separation performance under laboratory conditions, achieving high levels of CO_2/CH_4 and H_2S/CH_4 selectivity of 8 to 10 and 15 to 19, respectively, while maintaining CO_2 and H_2S permeability of 122 and 223 GPU (Table 10). For rubber polymers, the TFC membrane for acid gas removal is also applied to rubber polymers. Mohammadi et al. [118] reported a TFC membrane made of a PEUU supported on a porous Teflon substrate. The structure of the TFC is shown in the below SEM (Fig. 13(d)). The average thickness of the active layer is 25 μm. The membranes can withstand the upstream pressure of 30 bar without plasticization and also a variety of temperature ranges. The membrane showed an average permeance of 95 and 45 GPU for H_2S and CO_2, with the H_2S/CH_4 and CO_2/CH_4 selectivity of 43 and 16.

5 Membrane process for H_2S/CH_4 and CO_2/CH_4 separation

The membrane process is very important in the real deacidification of NG. Bhide and Stern [143] investigated the economic feasibility of asymmetric CA membranes for NG desulfurization, who designed seven different membrane separation processes and examined the effects of various process and economic parameters, including feed composition, flow rate, and pressure, membrane stage cut, pressure ratio, recovery rate, and the influence of membrane material selectivity on economic performance. Bhide and Stern [143] further investigated the economic feasibility of a hybrid process for acid gas separation that combines membrane separation with diethanolamine absorption. They examined the impact of various process and economic parameters on the total processing cost, and thereafter, selected two streams of feed gas at about 35 MMSCFD, the stream A is H_2S free and stream B contains H_2S of 5000 ppm, and the feed pressure was set at 800 psi to mimic the real NG

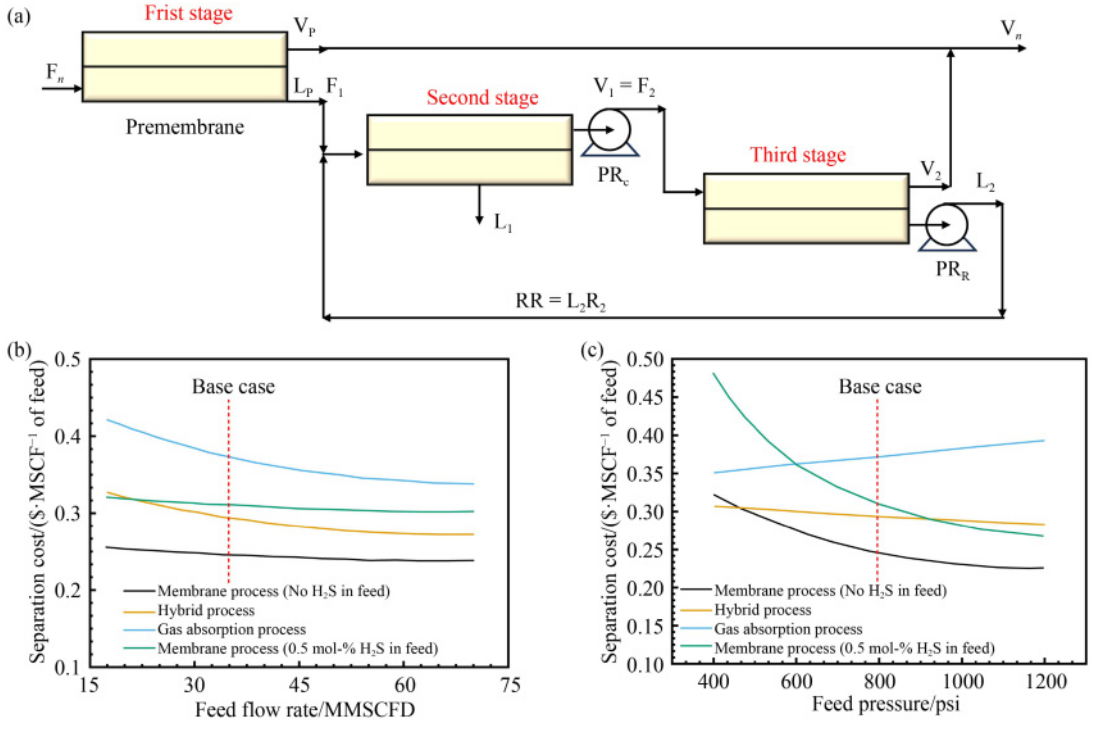

Fig. 14 (a) Illustration of a three-stage desulfurization process flow. Reprinted with permission from Ref. [144], copyright 1993, Elsevier. (b, c) Flow rate and feed pressure on the cost of the NG sweetening with hybrid system. Reprinted with permission from Ref. [144], copyright 1998, Elsevier.

condition. CTA was adopted as a membrane with H_2S/CH_4 and CO_2/CH_4 selectivity of 19 and 21, respectively. The membrane system used is a three-stage membrane system shown as follows (Fig. 14).

The result indicated that the total separation cost for the H_2S free feed is the lowest (0.244 \$·MMSCFD^{-1}). If there is H_2S in the feeding component, the hybrid system is the most energy efficient way to deacidification of the NG (0.296 \$·MMSCFD^{-1}). The author also investigated the feed flow rate and pressure on the cost of the acid gas removal from NG [144]. The result indicated that the hybrid system is very sensitive to the flow rate whereas the membrane system is highly dependent on the feed pressure of the system.

Hao et al. [145,146] studied the upgrading low-quality NG with two polymer membranes 6FDA-HAB and PEUU, the PEUU is H_2S selective (H_2S/CH_4 = 75) and the 6FDA-HAB is CO_2-selective (CO_2/CH_4 = 60). The NG component ratios studied is $CO_2/CH_4/H_2S$ (40/10/50) at the feed flow rate of 35 MMSCFD. Seven processes were proposed for this acid gas removal (Fig. 15). Under conditions without considering recycle flow, different gas compositions correspond to different process configurations. For instance, under conditions with a low amount of H_2S (≤ 10 mol %) and CO_2, the cost of using a single H_2S membrane is the lowest. In contrast, when CO_2 is present in medium amounts (≤ 40 mol %) whereas H_2S is low (≤ 8 ppm), the cost of a single CO_2 membrane is the lowest. However, when both H_2S (≤ 10 mol %) and CO_2 (≤ 40 mol %) are present in relatively low concentrations, a series of two-stage membranes is most suitable.

The impacts of recycle flow, feed flow rate, pressure variations, and membrane module costs on the processing costs of low-quality NG were also discussed. In the absence of recycle flow, the cost mainly depends on CH_4 loss. With recycle flow, for low acid gas content, the separation cost is influenced by CH_4 loss, whereas for higher acid gas content, the separation cost depends on the cost of gas recycling. The actual acid gas content also depends on the feed composition and operating conditions. Hao et al. [146] summarized the membrane separation costs for different $CH_4/CO_2/H_2S$ ratios, as shown in Fig. 15(f). In which, A represents a single-stage CO_2/CH_4 selective membrane. B represents two-stage membrane in series without recycle, first stage H_2S/CH_4 selective membrane and second stage CO_2/CH_4 selective membrane. C represents a single-stage H_2S/CH_4 selective membrane. D shows a two-stage membrane in series with recycle. For treating NG with 0–40 mol % CO_2 and 0–10 mol % H_2S to meet pipeline specifications for both acidic gases, different processes are required.

In 2011, Peters et al. [147] investigated amine absorption and membrane acidic gas removal using Aspen Hysys software and estimated the total capital investment for each system. For amine absorption, with an acid gas recovery rate of 90%, the purity of the acid gas was 98%. In membrane separation, the scheme of the membrane process is shown in Fig. 16, the performance of PVAm/PVA membranes was used to simulate the separation of acidic gases. Compared to amine absorption, the CO_2 produced by membrane separation

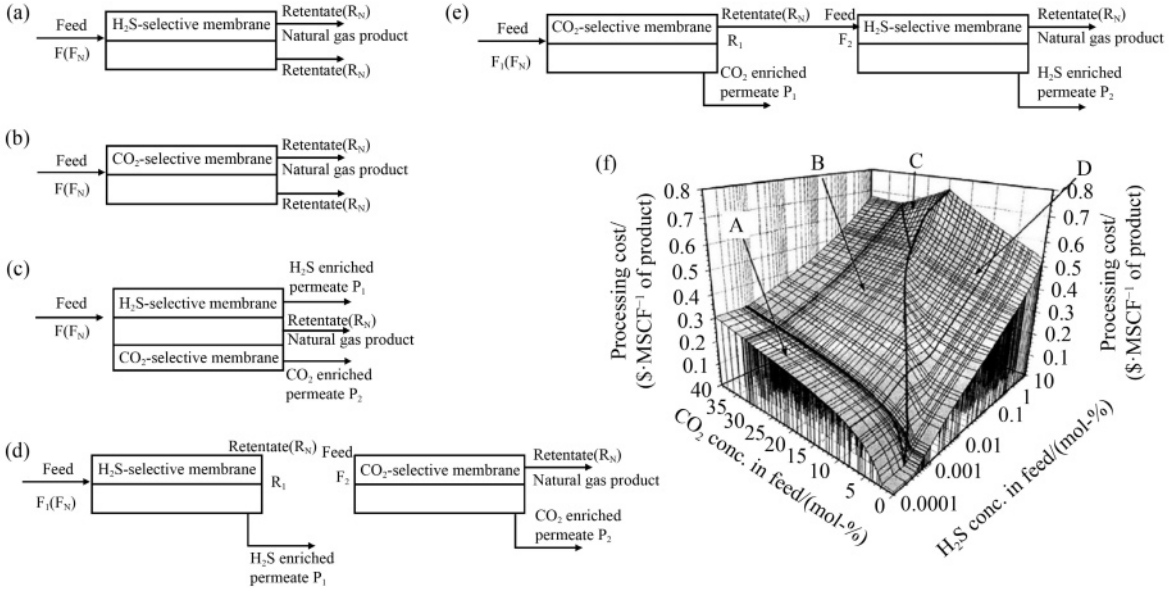

Fig. 15 Process flow diagram of membrane systems without recycle. (a) Single stage with H_2S-selective membranes. (b) Single stage with CO_2-selective membranes. (c) Single stage with both H_2S-and CO_2-selective membranes. (d) Two stages in series with H_2S-selective membranes in the first stage and CO_2-selective membranes in the second stage. (e) Two stages in series with CO_2-selective membranes in the first stage and H_2S -selective membranes in the second stage. Reprinted with permission from Ref. [146], copyright 2008, Elsevier. (f) Relationship between processing cost and the feed concentrations of CO_2 and H_2S. Reprinted with permission from Ref. [25], copyright 2015, Elsevier.

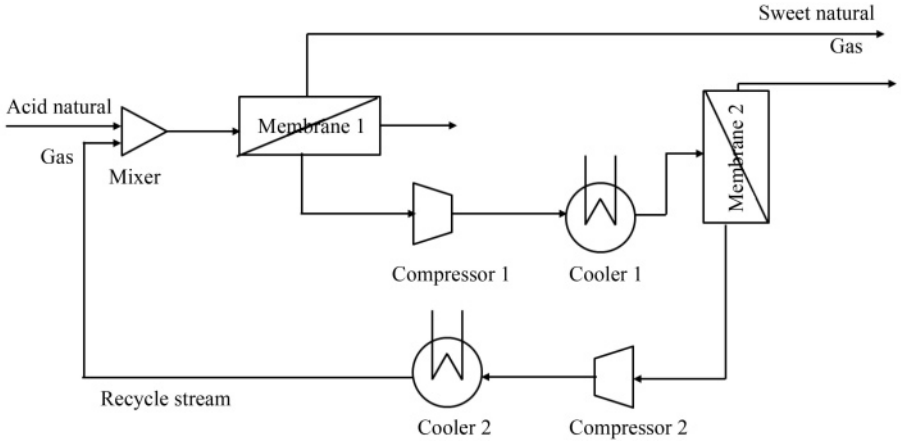

Fig. 16 Simplified flowsheet of a 2-stage membrane cascade with retentate recycle. Reprinted with permission from Ref. [147], copyright 2011, Elsevier.

meets the sales gas standards (< 2% CO_2 in the sales gas), but the CO_2 purity is lower than that produced by amine absorption. However, the cost of membrane-based acidic gas separation is lower.

Harasimowicz et al. [8] simulated the enrichment of CH_4 from biogas using a mixture of CH_4, CO_2, and H_2S. In this study, the test was conducted on an A-2 hollow fiber membrane module from UBE Europa GmbH. The feed gas flow rate was 0.2 $Nm^3 \cdot h^{-1}$, feed pressure was 0.60 MPa, retentate side pressure was 0.58 MPa, permeate was at atmospheric pressure, and the QP/QR ratio was 1:1, with temperatures ranging from 10 to 60 °C (Fig. 17(a)). The results indicated that using a capillary module with PI membranes could enrich the CH_4 concentration from 55%–85% to 91%–94.4%. The membrane material is resistant to low concentrations of acidic gases and ensures a reduction in H_2S and water vapor concentrations.

Seong et al. [148] reported on the design, construction, and optimization of a pilot-scale 3-stage membrane system operated by a single compressor, which was used for producing high-purity CH_4 and CO_2 from raw biogas. The effects of feed pressure and temperature on the gas separation performance of the developed membrane modules were explored. Additionally, the impact of various operating conditions on the purity and recovery rate of CH_4 was reported. Using simulation programs and gas permeation data, a 3-stage membrane system capable of processing 100 $Nm^3 \cdot h^{-1}$ of raw biogas (65–75 vol % CH_4) was designed and constructed (Fig. 17(b)). It was confirmed that the final purity and recovery rates of CH_4 and CO_2 obtained in the constructed 3-stage pilot plant were influenced by the operating conditions. Under optimized operating conditions, the 3-stage membrane system demonstrated excellent biogas separation performance, with high CH_4 purity and good recovery rates (98.4% and 98.7%, respectively), as well as high CO_2 purity and recovery rates (97.2% and 97.0%, respectively). This study demonstrated that a 3-stage pilot-scale system using PSF hollow fiber membranes can produce high-purity CH_4 and CO_2 from low-purity biogas simultaneously.

6 Conclusions and outlook

Membrane-based NG sweetening process has shown a great perspective in both energy saving and footprint reduction. Different membranes can be considered as potential candidates for CO_2 and H_2S removal simultaneously. Conventional polymers such as CTA, PPO, PSF, and PI membranes are excellent candidates due to their high robustness and reliability in real industrial gas separations. However, advanced membranes with higher CO_2 and H_2S permeance and CO_2/CH_4 as well as H_2S/CH_4 selective membrane should be developed.

The rubber polymers exhibited much higher H_2S permeability and H_2S/CH_4 selectivity than the conventional glassy polymers, however, the thin film formation ability of the rubber polymers still needs to be strengthened to get a better permeance for acid gas removal. Meanwhile, the combination of glassy polymers for CO_2 separation while using the rubber polymers for H_2S removal seems one of the best choices for efficiently removing both the CO_2 and H_2S in NS sweetening technique.

The PIM based polymers, especially the AO-PIM-1 has the best CO_2/CH_4 and H_2S/CH_4 separation performances, which is attributed to its highly rigid glassy polymer properties and large microporosity that ensure the high solubility selectivity of H_2S/CH_4, making this kind of polymers ideal for acid gas removal in NG. The CMSMs are also considered as potential for H_2S and CO_2 removal simultaneously. Both high permeability and selectivity as well as high pressure resistance make it a potential good candidate for NS gas purification.

The hollow fiber membrane is the only membrane format that practically used for NS deacidification, however, hollow fiber membrane procedure, excellent

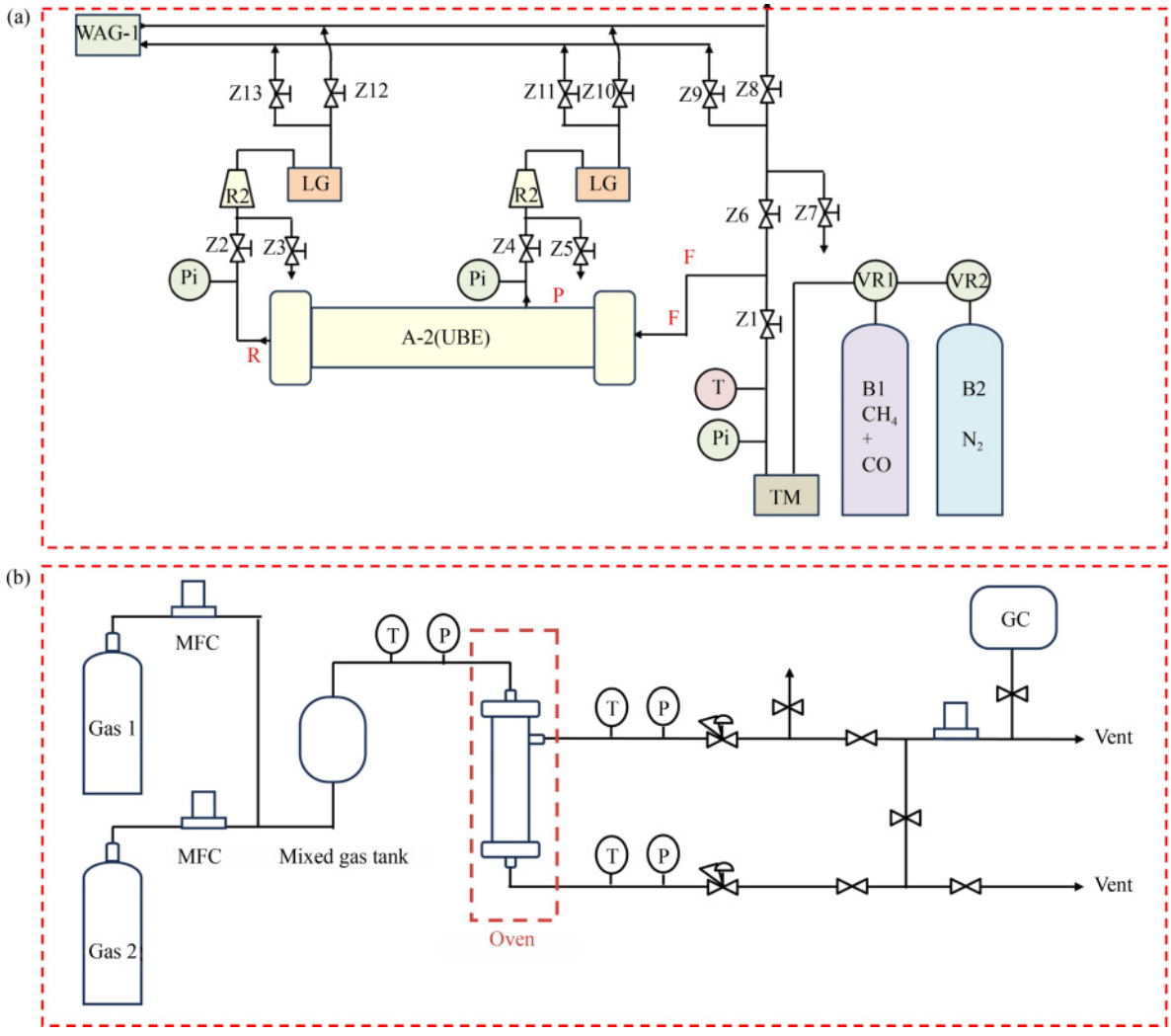

Fig. 17 (a) Schematic of the biogas sweetening using A-2(UBE) membrane module. Reprinted with permission from Ref. [8], copyright 2007, Elsevier. (b) Schematic diagram of gas separation for pure and mixed biogas deacidification. Reprinted with permission from Ref. [148], copyright 2019, Elsevier.

membrane materials are still need to be further developed. Additionally, thin-film composite membranes are also in great perspective in future H_2S removal applications. Furthermore, for a good membrane separation, the membrane process also needs to be optimized based on the properties of advanced membrane module.

Competing interests The authors declare that they have no competing interests.

Acknowledgements This work was supported by the National Natural Science Foundation of China (Grant Nos. 22078245 and 22378313), YLU-DNL Fund (Grant No. 2022009), we also great appreciate the support from Yiran Membrane (Hanzhou) Low Carbon Technique. Ltd.

References

1. Liu Q, Zhu D, Jin Z, Tian H, Zhou B, Jiang P, Meng Q, Wu X, Xu H, Hu T, et al. Carbon capture and storage for long-term and safe sealing with constrained natural CO_2 analogs. Renewable & Sustainable Energy Reviews, 2023, 171: 113000
2. Hanssen S V, Daioglou V, Steinmann Z J N, Doelman J C, Van Vuuren D P, Huijbregts M A J. The climate change mitigation potential of bioenergy with carbon capture and storage. Nature Climate Change, 2020, 10(11): 1023–1029
3. Li H, Zhao J, Zhang R, Hou B. The natural gas consumption and mortality nexus: a mediation analysis. Energy, 2022, 248: 123577
4. Hafezi R, Akhavan A, Pakseresht S A, Wood D. Global natural gas demand to 2025: a learning scenario development model. Energy, 2021, 224: 120167
5. Baker R W, Lokhandwala K. Natural gas processing with membranes: an overview. Industrial & Engineering Chemistry Research, 2008, 47(7): 2109–2121
6. Ma Y, Guo H, Selyanchyn R, Wang B, Deng L, Dai Z, Jiang X. Hydrogen sulfide removal from natural gas using membrane technology: a review. Journal of Materials Chemistry A: Materials for Energy and Sustainability, 2021, 9(36): 20211–20240
7. Boschee P. Taking on the technical challenges of sour gas

processing. Oil and Gas Facilities, 2014, 3(6): 21–25
8. Harasimowicz M, Orluk P, Zakrzewska-Trznadel G, Chmielewski A G. Application of polyimide membranes for biogas purification and enrichment. Journal of Hazardous Materials, 2007, 144(3): 698–702
9. Burgers W F J, Northrop P S, Kheshgi H S, Valencia J A. Worldwide development potential for sour gas. Energy Procedia, 2011, 4: 2178–2184
10. Aminuddin M S, Bustam M A, Johari K. Latest technological advances and insights into capture and removal of hydrogen sulfide: a critical review. RSC Sustainability, 2024, 2(4): 757–803
11. Reiffenstein R J, Hulbert W C, Roth S H. Toxicology of hydrogen sulfide. Annual Review of Pharmacology and Toxicology, 1992, 32(1): 109–134
12. Du Z, Liu C, Zhai J, Guo X, Xiong Y, Su W, He G. A review of hydrogen purification technologies for fuel cell vehicles. Catalysts, 2021, 11(3): 393
13. Qi M, Liu Y, He T, Yin L, Shu C M, Moon I. System perspective on cleaner technologies for renewable methane production and utilisation towards carbon neutrality: principles, techno-economics, and carbon footprints. Fuel, 2022, 327: 125130
14. Khan U, Ogbaga C C, Abiodun O A O, Adeleke A A, Ikubanni P P, Okoye P U, Okolie J A. Assessing absorption-based CO_2 capture: research progress and techno-economic assessment overview. Carbon Capture Science & Technology, 2023, 8: 100125
15. Scholes C A, Stevens G W, Kentish S E. Membrane gas separation applications in natural gas processing. Fuel, 2012, 96: 15–28
16. Rezakazemi M, Heydari I, Zhang Z. Hybrid systems: combining membrane and absorption technologies leads to more efficient acid gases (CO_2 and H_2S) removal from natural gas. Journal of CO_2 Utilization, 2017, 18: 362–369
17. Liu C, Greer D W, O'Leary B W. Advanced Materials and Membranes for Gas Separations: UOP Approach. Nanotechnology: Delivering on the Promise, 2016, 2: 119–135
18. Bernardo P, Tasselli F, Clarizia G. Gas separation hollow fiber membranes: processing conditions for manipulating morphology and performance. Chemical Engineering Transactions, 2013, 32: 1999–2004
19. Anderson C L. Case Study: Membrane CO_2 Removal From Natural Gas. Regional Symposium on Membrane Science & Technology, 2004.
20. Alcheikhhamdon Y, Hoorfar M. Natural gas purification from acid gases using membranes: a review of the history, features, techno-commercial challenges, and process intensification of commercial membranes. Chemical Engineering and Processing, 2017, 120: 105–113
21. Bettenhausen C. Evonik boosts gas separation membrane capacity. Chemical and Engineering News, 2021, 99(33): 14
22. Hasan R, Scholes C A, Stevens G W, Kentish S E. Effect of hydrocarbons on the separation of carbon dioxide from methane through a polyimide gas separation membrane. Industrial & Engineering Chemistry Research, 2009, 48(11): 5415–5419
23. Galizia M, Chi W S, Smith Z P, Merkel T C, Baker R W, Freeman B D. 50th anniversary perspective: polymers and mixed matrix membranes for gas and vapor separation: a review and prospective opportunities. Macromolecules, 2017, 50(20): 7809–7843
24. Brunetti A, Scura F, Barbieri G, Drioli E. Membrane technologies for CO_2 separation. Journal of Membrane Science, 2010, 359(1–2): 115–125
25. George G, Bhoria N, AlHallaq S, Abdala A, Mittal V. Polymer membranes for acid gas removal from natural gas. Separation and Purification Technology, 2016, 158: 333–356
26. Chen X, Liu G, Jin W. Natural gas purification by asymmetric membranes: an overview. Green Energy & Environment, 2021, 6(2): 176–192
27. Sanders D F, Smith Z P, Guo R, Robeson L M, McGrath J E, Paul D R, Freeman B D. Energy-efficient polymeric gas separation membranes for a sustainable future: a review. Polymer, 2013, 54(18): 4729–4761
28. Sun L, Xu Z, Huang L, Wang H, Zhang H, Li J, Wang Y, Ma X. Significantly enhanced gas separation properties of membranes by debromination and thermal rearrangement simultaneously. Journal of Membrane Science, 2024, 698: 122619
29. Weng Y, Li N, Xu Z, Huang J, Huang L, Wang H, Li J, Wang Y, Ma X. Super high gas separation performance membranes derived from a brominated alternative PIM by thermal induced crosslinking and carbonization at low temperature. Separation and Purification Technology, 2023, 314: 123548
30. Robeson L M. Correlation of separation factor versus permeability for polymeric membranes. Journal of Membrane Science, 1991, 62(2): 165–185
31. Baker R W. Membrane Technology and Applications. 2nd ed. Hoboken: John Wiley & Sons, 2004
32. Wijmans J G, Baker R W. The solution-diffusion model: a review. Journal of Membrane Science, 1995, 107(1–2): 1–21
33. Barrer R M. Diffusivities in glassy polymers for the dual mode sorption model. Journal of Membrane Science, 1984, 18: 25–35
34. Crank J. The Mathematic of Diffusion. Oxford: Oxford at the Clarendon Press, 1975
35. Yampolskii Y, Pinnau I, Freeman B. Materials Science of Membranes for Gas and Vapor Separation. Hoboken: John Wiley & Sons, 2006
36. Bondi A. van der Waals volumes and radii. Journal of Physical Chemistry, 1964, 68(3): 441–451
37. Freeman B D. Basis of permeability/selectivity tradeoff relations in polymeric gas separation membranes. Macromolecules, 1999, 32(2): 375–380
38. Robeson L M. The upper bound revisited. Journal of Membrane Science, 2008, 320(1–2): 390–400
39. Comesaña-Gándara B, Chen J, Bezzu C G, Carta M, Rose I, Ferrari M C, Esposito E, Fuoco A, Jansen J C, McKeown N B. Redefining the Robeson upper bounds for CO_2/CH_4 and CO_2/N_2 separations using a series of ultrapermeable benzotriptycene-based polymers of intrinsic microporosity. Energy & Environmental Science, 2019, 12(9): 2733–2740
40. Yi S, Ghanem B, Liu Y, Pinnau I, Koros W J. Ultraselective glassy polymer membranes with unprecedented performance for

energy-efficient sour gas separation. Science Advances, 2019, 5(5): eaaw5459
41. Hayek A, Shalabi Y A, Alsamah A. Sour mixed-gas upper bounds of glassy polymeric membranes. Separation and Purification Technology, 2021, 277: 119535
42. Kraftschik B, Koros W J, Johnson J R, Karvan O. Dense film polyimide membranes for aggressive sour gas feed separations. Journal of Membrane Science, 2013, 428: 608–619
43. Liu Y, Liu Z, Liu G, Qiu W, Bhuwania N, Chinn D, Koros W J. Surprising plasticization benefits in natural gas upgrading using polyimide membranes. Journal of Membrane Science, 2020, 593: 117430
44. Dong G, Li H, Chen V. Plasticization mechanisms and effects of thermal annealing of Matrimid hollow fiber membranes for CO_2 removal. Journal of Membrane Science, 2011, 369(1–2): 206–220
45. Bos A, Pünt I G M, Wessling M, Strathmann H. CO_2-induced plasticization phenomena in glassy polymers. Journal of Membrane Science, 1999, 155(1): 67–78
46. Minelli M, Oradei S, Fiorini M, Sarti G C. CO_2 plasticization effect on glassy polymeric membranes. Polymer, 2019, 163: 29–35
47. Low B T, Chung T S, Chen H, Jean Y C, Pramoda K P. Tuning the free volume cavities of polyimide membranes via the construction of pseudo-interpenetrating networks for enhanced gas separation performance. Macromolecules, 2009, 42(18): 7042–7054
48. Kratochvil A M, Koros W J. Decarboxylation-induced cross-linking of a polyimide for enhanced CO_2 plasticization resistance. Macromolecules, 2008, 41(21): 7920–7927
49. Qiu W L, Chen C C, Xu L R, Cui L L, Paul D R, Koros W J. Sub-T_g cross-linking of a polyimide membrane for enhanced CO_2 plasticization resistance for natural gas separation. Macromolecules, 2011, 44(15): 6046–6056
50. Rowe B W, Robeson L M, Freeman B D, Paul D R. Influence of temperature on the upper bound: theoretical considerations and comparison with experimental results. Journal of Membrane Science, 2010, 360(1–2): 58–69
51. Odian G. Principles of Polymerization. 4th ed. Hoboken: John Wiley & Sons, 2004
52. Klemm D, Heublein B, Fink H P, Bohn A. Cellulose: fascinating biopolymer and sustainable raw material. Angewandte Chemie International Edition, 2005, 44(22): 3358–3393
53. Bashir Z, Lock S S M, Hira N E, Ilyas S U, Lim L G, Lock I S M, Yiin C L, Darban M A. A review on recent advances of cellulose acetate membranes for gas separation. RSC Advances, 2024, 14(27): 19560–19580
54. Puleo A C, Paul D R, Kelley S S. The effect of degree of acetylation on gas sorption and transport behavior in cellulose acetate. Journal of Membrane Science, 1989, 47(3): 301–332
55. Schell W J, Wensley C G, Chen M S K, Venugopal K G, Miller B D, Stuart J A. Recent advances in cellulosic membranes for gas separation and pervaporation. Gas Separation & Purification, 1989, 3(4): 162–169
56. Chatterjee G, Houde A A, Stern S A. Poly(ether urethane) and poly(ether urethane urea) membranes with high H_2S/CH_4 selectivity. Journal of Membrane Science, 1997, 135(1): 99–106
57. Achoundong C S K, Bhuwania N, Burgess S K, Karvan O, Johnson J R, Koros W J. Silane modification of cellulose acetate dense films as materials for acid gas removal. Macromolecules, 2013, 46(14): 5584–5594
58. Peters T A, Ansaloni L, Tena A, Karvan O, Visser T, Chinn D, Bhuwania N. Performance and stability of cellulose triacetate membranes in humid high H_2S natural gas feed streams. Journal of Membrane Science, 2024, 693: 122324
59. Aldhawi Z A. BinSharfan I I, Abdulhamid M A. Chapter 1 Polyimide-based membranes for gas separation applications. In: Polymer Membranes: Increasing Energy Efficiency. Boston: De Gruyter, 2024: 1–44
60. Ma X H, Yang S Y. Polyimide Gas Separation Membranes. In: Advanced Polyimide Materials. Amsterdam: Elsevier, 2018: 257–322
61. Wang Y, Alaslai N, Ghanem B, Ma X, Hu X, Balcik M, Liu Q, Abdulhamid M A, Han Y, Eddaoudi M, et al. Hydroxyl-functionalized polymers of intrinsic microporosity and dual-functionalized blends for high-performance membrane-based gas separations. Advanced Materials, 2024, 36(51): 2406076
62. Guo W, Sun L, Chu J, Liu L, Li J, Ma X. Huge improved gas separation performance of carbon molecular sieve membrane by forming a double crosslinked polyimide precursor. Journal of Membrane Science, 2024, 711: 123218
63. Chen J, Cai M, Han Z, Chen Z, Sun L, Liu H, Zhang S, Cui T, Min Y. Ultra-high selectivity carbon molecular sieve membrane derived from PI/SPANI blends for efficient gas separation. Separation and Purification Technology, 2025, 354: 128797
64. Ye C, Luo C, Ji W, Weng Y, Li J, Yi S, Ma X. Significantly enhanced gas separation properties of microporous membranes by precisely tailoring their ultra-microporosity through bromination/debromination. Chemical Engineering Journal, 2023, 451: 138513
65. Zhao W, Li K, Ma Y, Gao Y, Zhang J, Zhou L, Wang W, Wang J, Ma Y, Guo M, et al. Simultaneously enhanced gas separation and anti-aging performance of intrinsic microporous polyimide by dibromo substitution. Journal of Membrane Science, 2023, 687: 122081
66. Zhao W, Zhang J, Liu C, Ma Y, Li K, Guo M, Jiao L, Ma X, Yang L, Yang S, et al. Fine-tuning gas separation performance of intrinsic microporous polyimide by the regulation of atomic-level halogen substitution. Journal of Membrane Science, 2024, 692: 122317
67. Ma X H, Abdulhamid M, Miao X H, Pinnau I. Facile synthesis of a hydroxyl-functionalized Tröger's base diamine: a new building block for high-performance polyimide gas separation membranes. Macromolecules, 2017, 50(24): 9569–9576
68. Ma X H, Abdulhamid M A, Pinnau I. Design and synthesis of polyimides based on carbocyclic Pseudo-Tröger's base-derived dianhydrides for membrane gas separation applications. Macromolecules, 2017, 50(15): 5850–5857
69. Zhang S, Xu Z, Weng Y, Cai M, Wang Y, Zhu W, Min Y, Ma X. Remarkable gas separation performance of a thermally rearranged membrane derived from an alkynyl self-crosslinkable precursor. Journal of Membrane Science, 2023, 672: 121464

70. White L S, Blinka T A, Kloczewski H A, Wang I F. Properties of a polyimide gas separation membrane in natural gas streams. Journal of Membrane Science, 1995, 103(1–2): 73–82
71. Tanaka K, Kita H, Okamoto K, Nakamura A, Kusuki Y. Gas permeability and permselectivity in polyimides based on 3,3′,4,4′-biphenyltetracarboxylic dianhydride. Journal of Membrane Science, 1989, 47(1–2): 203–215
72. Tanaka K, Okano M, Toshino H, Kita H, Okamoto K I. Effect of methyl substituents on permeability and permselectivity of gases in polyimides prepared from methyl-substituted phenylenediamines. Journal of Polymer Science. Part B, Polymer Physics, 1992, 30(8): 907–914
73. Vaughn J T, Koros W J, Johnson J R, Karvan O. Effect of thermal annealing on a novel polyamide-imide polymer membrane for aggressive acid gas separations. Journal of Membrane Science, 2012, 401–402: 163–174
74. Vaughn J T, Koros W J. Analysis of feed stream acid gas concentration effects on the transport properties and separation performance of polymeric membranes for natural gas sweetening: a comparison between a glassy and rubbery polymer. Journal of Membrane Science, 2014, 465: 107–116
75. Yahaya G O, Qahtani M S, Ammar A Y, Bahamdan A A, Ameen A W, Alhajry R H, Sultan M M B, Hamad F. Aromatic block co-polyimide membranes for sour gas feed separations. Chemical Engineering Journal, 2016, 304: 1020–1030
76. Yahaya G O, Hayek A, Alsamah A, Shalabi Y A, Ben Sultan M M, Alhajry R H. Copolyimide membranes with improved H_2S/CH_4 selectivity for high-pressure sour mixed-gas separation. Separation and Purification Technology, 2021, 272: 118897
77. Yahaya G O, Mokhtari I, Alghannam A A, Choi S H, Maab H, Bahamdan A A. Cardo-type random co-polyimide membranes for high pressure pure and mixed sour gas feed separations. Journal of Membrane Science, 2018, 550: 526–535
78. Alghannam A A, Yahaya G O, Hayek A, Mokhtari I, Saleem Q, Sewdan D A, Bahamdan A A. High pressure pure- and mixed sour gas transport properties of Cardo-type block co-polyimide membranes. Journal of Membrane Science, 2018, 553: 32–42
79. Hayek A, Yahaya G O, Alsamah A, Panda S K. Fluorinated copolyimide membranes for sour mixed-gas upgrading. Journal of Applied Polymer Science, 2019, 137(5): 48336
80. Ghanem B S, McKeown N B, Budd P M, Selbie J D, Fritsch D. High-performance membranes from polyimides with intrinsic microporosity. Advanced Materials, 2008, 20(14): 2766–2771
81. Lee M, Bezzu C G, Carta M, Bernardo P, Clarizia G, Jansen J C, McKeown N B. Enhancing the gas permeability of Tröger's base derived polyimides of intrinsic microporosity. Macromolecules, 2016, 49(11): 4147–4154
82. Hayek A, Yahaya G O, Alsamah A, Alghannam A A, Jutaily S A, Mokhtari I. Pure- and sour mixed-gas transport properties of 4,4′-methylenebis(2,6-diethylaniline)-based copolyimide membranes. Polymer, 2019, 166: 184–195
83. Hayek A, Alsamah A, Qasem E A, Alaslai N, Alhajry R H, Yahaya G O. Effect of pendent bulky groups on pure- and sour mixed-gas permeation properties of triphenylamine-based polyimides. Separation and Purification Technology, 2019, 227: 115713
84. Hayek A, Alsamah A, Yahaya G O, Qasem E A, Alhajry R H. Post-synthetic modification of CARDO-based materials: application in sour natural gas separation. Journal of Materials Chemistry. A, Materials for Energy and Sustainability, 2020, 8(44): 23354–23367
85. Hayek A, Alsamah A, Saleem Q, Alhajry R H, Alsuwailem A A, Jassim F I. Modified CARDO-based copolyimides with improved sour mixed-gas permeation properties. ACS Applied Polymer Materials, 2022, 4(12): 9257–9271
86. Liu Z, Liu Y, Qiu W, Koros W J. Molecularly engineered 6FDA-based polyimide membranes for sour natural gas separation. Angewandte Chemie International Edition, 2020, 59(35): 14877–14883
87. Kraftschik B, Koros W J. Cross-linkable polyimide membranes for improved plasticization resistance and permselectivity in sour gas separations. Macromolecules, 2013, 46(17): 6908–6921
88. Budd P M, Ghanem B S, Makhseed S, McKeown N B, Msayib K J, Tattershall C E. Polymers of intrinsic microporosity (PIMs): robust, solution-processable, organic nanoporous materials. Chemical Communications, 2004(2): 230–231
89. Rose I, Bezzu C G, Carta M, Comesana-Gandara B, Lasseuguette E, Ferrari M C, Bernardo P, Clarizia G, Fuoco A, Jansen J C, et al. Polymer ultrapermeability from the inefficient packing of 2D chains. Nature Materials, 2017, 16(9): 932–937
90. Carta M, Malpass-Evans R, Croad M, Rogan Y, Jansen J C, Bernardo P, Bazzarelli F, McKeown N B. An efficient polymer molecular sieve for membrane gas separations. Science, 2013, 339(6117): 303–307
91. Lai H W H, Benedetti F M, Ahn J M, Robinson A M, Wang Y, Pinnau I, Smith Z P, Xia Y. Hydrocarbon ladder polymers with ultrahigh permselectivity for membrane gas separations. Science, 2022, 375(6587): 1390–1392
92. Chen L, Han X, Chen G, Sun R, Li W, Lin Z, Pang J, Jiang Z. A structure-property study for the effect of methyl substituents on the gas separation of spirodifluoranthene-based polymers of intrinsic microporosity. Journal of Membrane Science, 2023, 683: 121817
93. Chen L, Li W, Chen G, Lin Z, Pang J, Jiang Z. *In situ* hydrolyzed microporous polymer membranes for additional free volume to facilitate CO_2 permeation. Journal of Membrane Science, 2025, 713: 123379
94. Sun L, Xu W, Zhang H, Chu J, Wang M, Song K, Wu W, Li J, Wang Y, Wang Y, et al. *In-situ* formation of three-dimensional network intrinsic microporous ladder polymer membranes with ultra-high gas separation performance and anti-trade-off effect. Angewandte Chemie International Edition, 2025, 64: e202420742
95. Yu C, Wang Y, Xia Y, Luo S, Ma X, Yin B H, Wang X. Polymers of intrinsic microporosity with internal dihedral lock for efficient gas separation. Advanced Membranes, 2024, 4: 100097
96. Masuda T, Isobe E, Hamano T. Synthesis of poly[1-(trimethylsilyl)-1-propyne] with extremely high molecular weight by using tantalum pentachloride-triphenylbismuth (1:1) catalyst. Macromolecules. 1986, 19(9): 2448–2450.

97. Merkel T. Mixed-gas permeation of syngas components in poly(dimethylsiloxane) and poly(1-trimethylsilyl-1-propyne) at elevated temperatures. Journal of Membrane Science, 2001, 191(1–2): 85–94
98. Malykh O V, Golub A Y, Teplyakov V V. Polymeric membrane materials: new aspects of empirical approaches to prediction of gas permeability parameters in relation to permanent gases, linear lower hydrocarbons and some toxic gases. Advances in Colloid and Interface Science, 2011, 164(1–2): 89–99
99. Yi S L, Ma X H, Pinnau I, Koros W J. A high-performance hydroxyl-functionalized polymer of intrinsic microporosity for an environmentally attractive membrane-based approach to decontamination of sour natural gas. Journal of Materials Chemistry A: Materials for Energy and Sustainability, 2015, 3(45): 22794–22806
100. Mizrahi Rodriguez K, Dean P A, Guo S, Roy N, Swager T M, Smith Z P. Elucidating the role of micropore-generating backbone motifs and amine functionality on membrane separation performance in complex mixtures. Journal of Membrane Science, 2024, 696: 122464
101. Dean P A, Mizrahi Rodriguez K, Guo S, Roy N, Swager T M, Smith Z P. Elucidating the role of micropore-generating backbone motifs and amine functionality on H_2S, CO_2, CH_4, and N_2 sorption. Journal of Membrane Science, 2024, 696: 122465
102. Dean P A, Wu Y, Guo S, Swager T M, Smith Z P. Tertiary-amine-functional poly(arylene ether)s for acid-gas separations. JACS Au, 2024, 4(10): 3848–3856
103. Park H B, Jung C H, Lee Y M, Hill A J, Pas S J, Mudie S T, Van Wagner E, Freeman B D, Cookson D J. Polymers with cavities tuned for fast selective transport of small molecules and ions. Science, 2007, 318(5848): 254–258
104. Yerzhankyzy A, Ghanem B S, Wang Y, Alaslai N, Pinnau I. Gas separation performance and mechanical properties of thermally-rearranged polybenzoxazoles derived from an intrinsically microporous dihydroxyl-functionalized triptycene diamine-based polyimide. Journal of Membrane Science, 2020, 595: 117512
105. Zhuang Y B, Seong J G, Lee W H, Do Y S, Lee M J, Wang G, Guiver M D, Lee Y M. Mechanically tough, thermally rearranged (TR) random/block poly(benzoxazole-co-imide) gas separation membranes. Macromolecules, 2015, 48(15): 5286–5299
106. Calle M, Jo H J, Doherty C M, Hill A J, Lee Y M. Cross-linked thermally rearranged poly(benzoxazole-co-imide) membranes prepared fromortho-hydroxycopolyimides containing pendant carboxyl groups and gas separation properties. Macromolecules, 2015, 48(8): 2603–2613
107. Cai M, Chen J, Liu H, Sun L, Wu J, Cui T, Zhang S, Ma X, Min Y. Unveiling the mystery: how TR precursors lead to exceptional gas separation performance in CMSMs. Journal of Membrane Science, 2025, 713: 123287
108. Cai M, Chen J, Liu H, Sun L, Wu J, Han Z, Chen Z, Cui T, Zhang S, Ma X, et al. Remarkably enhanced molecular sieving effect of carbon molecular sieve membrane by enhancing the concentration of thermally rearranged precursors. Separation and Purification Technology, 2024, 341: 126945
109. Cai M, Liu H, Chen J, Sun L, Wu J, Chen Z, Han Z, Cui T, Zhang S, Min Y, et al. Breaking the permeability-selectivity trade-off: advanced carbon molecular sieve membranes derived from thermally rearranged mixed-matrix membrane precursors. Separation and Purification Technology, 2024, 335: 126163
110. Sun L, Chu J, Zuo H, Wang M, Wu C, Riaz A, Liu L, Guo W, Li J, Ma X. The influence of debromination and TR on the microstructure and properties of CMSMs. Separation and Purification Technology, 2025, 352: 128167
111. Scholes C A, Dong G, Kim J S, Jo H J, Lee J, Lee Y M. Permeation and separation of SO_2, H_2S and CO_2 through thermally rearranged (TR) polymeric membranes. Separation and Purification Technology, 2017, 179: 449–454
112. Ghasemnejad-Afshar E, Amjad-Iranagh S, Zarif M, Modarress H. Effect of side branch on gas separation performance of triptycene based PIM membrane: a molecular simulation study. Polymer Testing, 2020, 83: 106339
113. Hayek A, Alsamah A, Alaslai N, Maab H, Qasem E A, Alhajry R H, Alyami N M. Unprecedented sour mixed-gas permeation properties of fluorinated polyazole-based membranes. ACS Applied Polymer Materials, 2020, 2(6): 2199–2210
114. Lawrence J A III, Harrigan D J, Maroon C R, Sharber S A, Long B K, Sundell B J. Promoting acid gas separations via strategic alkoxysilyl substitution of vinyl-added poly(norbornene)s. Journal of Membrane Science, 2020, 616: 118569
115. Merkel T C, Toy L G. Comparison of hydrogen sulfide transport properties in fluorinated and nonfluorinated polymers. Macromolecules, 2006, 39(22): 7591–7600
116. Signorini V, Giacinti Baschetti M, Pizzi D, Merlo L. Permeation of ternary mixture containing H_2S, CO_2 and CH_4 in Aquivion® perfluorosulfonic acid (PFSA) ionomer membranes. Membranes, 2022, 12(11): 1034
117. Sadeghi M, Talakesh M M, Arabi Shamsabadi A, Soroush M. Novel application of a polyurethane membrane for efficient separation of hydrogen sulfide from binary and ternary gas mixtures. ChemistrySelect, 2018, 3(11): 3302–3308
118. Mohammadi T, Moghadam M T, Saeidi M, Mahdyarfar M. Acid gas permeation behavior through poly(ester urethane urea) membrane. Industrial & Engineering Chemistry Research, 2008, 47(19): 7361–7367
119. Harrigan D J, Lawrence J A III, Reid H W, Rivers J B, O'Brien J T, Sharber S A, Sundell B J. Tunable sour gas separations: simultaneous H_2S and CO_2 removal from natural gas via crosslinked telechelic poly(ethylene glycol) membranes. Journal of Membrane Science, 2020, 602: 117947
120. Harrigan D J, Yang J, Sundell B J, Lawrence J A III, O'Brien J T, Ostraat M L. Sour gas transport in poly(ether-b-amide) membranes for natural gas separations. Journal of Membrane Science, 2020, 595: 117497
121. Wong D A, Haddad E E, Lin S, Sharber S A, Yang J, Lawrence J A III, Harrigan D J, Wright P T, Liu Y, Sundell B J. Rational design of melamine-crosslinked poly(ethylene glycol) membranes for sour gas purification. Journal of Membrane Science, 2024, 709: 123082
122. Zhang P, Ma X, Tu Z, Zhang X, Hu X, Wu Y. Constructing ether-rich and carboxylate hydrogen bonding sites in protic ionic

liquids for efficient and simultaneous membrane separation of H_2S and CO_2 from CH_4. Green Energy & Environment, 2024, 10(3): 560–572

123. Zhang C, Koros W J. Ultraselective carbon molecular sieve membranes with tailored synergistic sorption selective properties. Advanced Materials, 2017, 29(33): 1701631
124. Sanyal O, Hays S S, Leon N E, Guta Y A, Itta A K, Lively R P, Koros W J. A Self-consistent model for sorption and transport in polyimide-derived carbon molecular sieve gas separation membranes. Angewandte Chemie International Edition, 2020, 59(46): 20343–20347
125. Hazazi K, Wang Y, Ghanem B, Hu X, Puspasari T, Chen C, Han Y, Pinnau I. Precise molecular sieving of ethylene from ethane using triptycene-derived submicroporous carbon membranes. Nature Materials, 2023, 22(10): 1218–1226
126. Shiflett M B, Foley H C. Ultrasonic deposition of high-selectivity nanoporous carbon membranes. Science, 1999, 285(5435): 1902–1905
127. Hu L, Bui V T, Krishnamurthy A, Fan S, Guo W, Pal S, Chen X, Zhang G, Ding Y, Singh R P, et al. Tailoring sub-3.3 Å ultramicropores in advanced carbon molecular sieve membranes for blue hydrogen production. Science Advances, 2022, 8(10): eabl8160
128. Enrico D, Giuseppe B, Enrico D, Giuseppe B. Membrane Engineering for the Treatment of Gases: Gas-separation Problems with Membranes. United Kingdom: The Royal Society of Chemistry, 2011.
129. Wu Z. Membrane Separation Principles and Applications. Amsterdam: Elsevier, 2019
130. Tronci G, Raffone F, Cicero G. Theoretical study of nanoporous graphene membranes for natural gas purification. Applied Sciences, 2018, 8(9): 1547
131. Haider S, Lindbråthen A, Lie J A, Hägg M B. Regenerated cellulose based carbon membranes for CO_2 separation: durability and aging under miscellaneous environments. Journal of Industrial and Engineering Chemistry, 2019, 70: 363–371
132. Li G, Kujawski W, Válek R, Koter S. A review —the development of hollow fibre membranes for gas separation processes. International Journal of Greenhouse Gas Control, 2021, 104: 103195
133. Morisato A, Mahley E. Hydrogen sulfide permeation and hydrocarbon separation properties in cellulose triacetate hollow fiber membrane for high hydrogen sulfide contained natural gas sweetening applications. Journal of Membrane Science, 2023, 681: 121734
134. Lu H T, Liu L, Kanehashi S, Scholes C A, Kentish S E. The impact of toluene and xylene on the performance of cellulose triacetate membranes for natural gas sweetening. Journal of Membrane Science, 2018, 555: 362–368
135. Niknejad S M S, Savoji H, Pourafshari Chenar M, Soltanieh M. Separation of H_2S from CH_4 by polymeric membranes at different H_2S concentrations. International Journal of Environmental Science and Technology, 2017, 14(2): 375–384
136. Chenar M P, Savoji H, Soltanieh M, Matsuura T, Tabe S. Removal of hydrogen sulfide from methane using commercial polyphenylene oxide and Cardo-type polyimide hollow fiber membranes. Korean Journal of Chemical Engineering, 2011, 28(3): 902–913
137. Saedi S, Madaeni S S, Shamsabadi A A. PDMS coated asymmetric PES membrane for natural gas sweetening: effect of preparation and operating parameters on performance. Canadian Journal of Chemical Engineering, 2014, 92(5): 892–904
138. Liu Z, Liu Y, Liu G, Qiu W, Koros W J. Cross-linkable semi-rigid 6FDA-based polyimide hollow fiber membranes for sour natural gas purification. Industrial & Engineering Chemistry Research, 2020, 59(12): 5333–5339
139. Liu Y, Liu Z, Kraftschik B E, Babu V P, Bhuwania N, Chinn D, Koros W J. Natural gas sweetening using TEGMC polyimide hollow fiber membranes. Journal of Membrane Science, 2021, 632: 119361
140. Shalabi Y A, Yahaya G O, Choi S H, Alsamah A, Hayek A. Copolyimide asymmetric hollow fiber membranes for high‐pressure natural gas purification. Journal of Applied Polymer Science, 2023, 140(21): e53866
141. Yahaya G O, Choi S H, Sultan M M B, Hayek A. Development of thin-film composite membranes from aromatic Cardo-type co-polyimide for mixed and sour gas separations from natural gas. Global Challenges, 2020, 4(7): 1900107
142. Liu Y, Liu Z, Morisato A, Bhuwania N, Chinn D, Koros W J. Natural gas sweetening using a cellulose triacetate hollow fiber membrane illustrating controlled plasticization benefits. Journal of Membrane Science, 2020, 601: 117910
143. Bhide B, Stern S A. Membrane processes for the removal of acid gases from natural gas. I. Process configurations and optimization of operating conditions. Journal of Membrane Science, 1993, 81(3): 209–237
144. Bhide B, Voskericyan A, Stern S. Hybrid processes for the removal of acid gases from natural gas. Journal of Membrane Science, 1998, 140(1): 27–49
145. Hao J, Rice P, Stern S. Upgrading low-quality natural gas with H_2S-and CO_2-selective polymer membranes: Part I. Process design and economics of membrane stages without recycle streams. Journal of Membrane Science, 2002, 209(1): 177–206
146. Hao J, Rice P, Stern S. Upgrading low-quality natural gas with H_2S-and CO_2-selective polymer membranes: Part II. Process design, economics, and sensitivity study of membrane stages with recycle streams. Journal of Membrane Science, 2008, 320(1–2): 108–122
147. Peters L, Hussain A, Follmann M, Melin T, Hägg M B. CO_2 removal from natural gas by employing amine absorption and membrane technology: a technical and economical analysis. Chemical Engineering Journal, 2011, 172(2–3): 952–960
148. Seong M S, Kong C I, Park B R, Lee Y, Na B K, Kim J H. Optimization of pilot-scale 3-stage membrane process using asymmetric polysulfone hollow fiber membranes for production of high-purity CH_4 and CO_2 from crude biogas. Chemical Engineering Journal, 2020, 384: 123342